

1 **OPENPichia: building a free-to-operate *Komagataella phaffii***

2 **protein expression toolkit**

3 Dries Van Herpe^{1,2,3*}, Robin Vanluchene^{1,2*}, Kristof Vandewalle^{1,2}, Sandrine Vanmarcke^{1,2}, Elise
4 Wyseure^{1,2}, Berre Van Moer^{1,2}, Hannah Eeckhaut^{1,2}, Daria Fijalkowska^{1,2}, Hendrik Grootaert^{1,2},
5 Chiara Lonigro^{1,2}, Leander Meuris^{1,2}, Gitte Michielsen^{1,2}, Justine Naessens^{1,2}, Charlotte Roels^{1,2},
6 Loes van Schie^{1,2}, Riet De Rycke^{4,5}, Michiel De Bruyne^{4,5}, Peter Borghgraef⁵, Katrien Claes^{1,2**}
7 and Nico Callewaert^{1,2**}

8 ¹Unit for Medical Biotechnology, Center for Medical Biotechnology, VIB, Technologiepark 75, 9052 Ghent,
9 Belgium.

10 ²Department of Biochemistry and Microbiology, Ghent University, K.L.-Ledeganckstraat 35, 9000 Ghent,
11 Belgium.

12 ³Inbiose NV, Ghent, Belgium.

13 ⁴Department of Biomedical Molecular Biology, Ghent University, Ghent, Belgium.

14 ⁵BioImaging Core, VIB, Technologiepark 71, 9052 Ghent, Belgium.

15

16 * These authors contributed equally to this manuscript.

17 **Correspondence should be addressed to N.C. (Nico.Callewaert@vib-ugent.be) and
18 K.C (Katrien.Claes@vib-ugent.be).

19

20

Abstract

21 In the standard toolkit for recombinant protein expression, the yeast known in biotechnology as
22 *Pichia pastoris* (formally: *Komagataella phaffii*) takes up the position between *E. coli* and HEK293
23 or CHO mammalian cells, and is used by thousands of laboratories both in academia and industry.
24 The organism is eukaryotic yet microbial, and grows to extremely high cell densities while
25 secreting proteins into its fully defined growth medium, using very well established strong
26 inducible or constitutive promoters. Many products made in *Pichia* are in the clinic and in industrial
27 markets. *Pichia* is also a favoured host for the rapidly emerging area of ‘precision fermentation’
28 for the manufacturing of food proteins. However, the earliest steps in the development of the
29 industrial strain (NRRL Y-11430/CBS 7435) that is used throughout the world were performed
30 prior to 1985 in industry (Phillips Petroleum Company) and are not in the public domain. Moreover,
31 despite the long expiry of associated patents, the patent deposit NRRL Y-11430/CBS 7435 that
32 is the parent to all commonly used industrial strains, is not or no longer made freely available
33 through the resp. culture collections. This situation is far from ideal for what is a major chassis for
34 synthetic biology, as it generates concern that novel applications of the system are still
35 encumbered by licensing requirements of the very basic strains. In the spirit of open science and
36 freedom to operate for what is a key component of biotechnology, we set out to resolve this by
37 using genome sequencing of type strains, reverse engineering where necessary, and
38 comparative protein expression and strain characterisation studies. We find that the industrial
39 strains derive from the *K. phaffii* type strain lineage deposited as 54-11.239 in the UC Davis Phaff
40 Yeast Strain collection by Herman Phaff in 1954. This type strain has valid equivalent deposits
41 that are replicated/derived from it in other yeast strain collections, incl. in ARS-NRRL NRRL
42 YB-4290 (deposit also made by Herman Phaff) and NRRL Y-7556, CBS 2612 and NCYC 2543.
43 We furthermore discovered that NRRL Y-11430 and its derivatives carry an ORF-truncating
44 mutation in the *HOC1* cell wall synthesis gene, and that reverse engineering of a similar mutation
45 in the NCYC 2543 type strain imparts the high transformability that is characteristic of the industrial
46 strains. Uniquely, the NCYC 2543 type strain, which we propose to call ‘OPENPichia’ henceforth,
47 is freely available from the NCYC culture collection, incl. resale and commercial production
48 licenses at nominal annual licensing fees¹. Furthermore, our not-for-profit research institute VIB
49 has also acquired a resale/distribution license from NCYC, which we presently use to openly
50 provide to end-users our genome-sequenced OPENPichia subclone strain and its derivatives,
51 i.e., currently the highly transformable *hoc1^{tr}* and the *his4* auxotrophic mutants. To complement
52 the OPENPichia platform, a fully synthetic modular gene expression vector building toolkit was
53 developed, which is also openly distributed, for any purpose. We invite other researchers to
54 contribute to our open science resource-building effort to establish a new unencumbered standard
55 chassis for *Pichia* synthetic biology.

56 **Introduction**

57 Presently, a wide variety of microbial hosts is available for the production of recombinant proteins.
58 However, for general laboratory use as well as biopharmaceutical protein manufacturing, a strong
59 consolidation has taken place over the past years. *E. coli* remains the most-frequently used
60 prokaryotic system for proteins of prokaryotic origin and for relatively simple stably folding proteins
61 of eukaryotic origin, especially those with no or few disulphide bonds. On the other end, production
62 in HEK293 or CHO cells is used for production of proteins of higher eukaryotic origin, affording
63 *i.a.* complex-type N-glycosylation. The methylotrophic yeast known in biotechnology as *Pichia*
64 *pastoris* (and formally classified as *Komagataella phaffii*) takes up the intermediate-complexity
65 position in most protein expression lab's toolkit, as it combines the easy cultivation and fast growth
66 of a micro-organism with the presence of a eukaryotic secretory system and the ensuing ability to
67 perform complex post-translational modifications such as N-glycosylation and strong capacity for
68 the formation and isomerization of disulphide bonds²⁻⁴. Hundreds of papers are published every
69 year reporting on the use of *Pichia* for protein production (and increasingly also for engineered
70 metabolite production, incl. in the area of sustainable chemical building block manufacturing from
71 methanol and even CO₂⁵). Quite often, *Pichia*-produced proteins are developed by academic and
72 industrial scientists alike with an eventual applied/commercial use in mind, being it as a
73 therapeutic compound, an industrial biocatalyst^{6,7} or more recently, as a food ingredient.

74 Historically, in 1954 Herman Phaff deposited a methylotrophic yeast strain from a black oak tree
75 (*Quercus*) in the Yosemite region⁸. The isolate was stored in the culture collection of the University
76 of California at Davis as UCD-FST K-239, with formally equivalent type strain deposits in other
77 culture collections as NRRL YB-4290, NRRL Y-7556, CBS 2612 and NCYC 2543. At this time,
78 these isolated strains of Phaff could not be distinguished from similar strains isolated in 1919 by
79 A. Guilliermond, and Herman Phaff categorized both together as a new species: *Pichia pastoris*
80 (the genus *Pichia* was established half a century before, in 1904, by E. Hanssen⁹) (Figure 1). In
81 1995, *Pichia pastoris* was re-classified into the new genus of *Komagataella*, named after the
82 Japanese scientist Kazuo Komagata as a tribute to his contributions to yeast systematics, in
83 particular the methanol-assimilating yeasts¹⁰. In 2005, the two distinctly evolved isolates from
84 Phaff and Guilliermond were divided into two separate species and renamed *Komagataella phaffii*
85 and *Komagataella pastoris* by C. Kurtzman¹¹, based on the sequencing of 26S rDNA.
86 Consequently, the strain of Phaff (UCD-FST K-239, NRRL YB-4290, NRRL Y- 7556, CBS 2612,
87 and NCYC 2543) was now considered the type strain of the species *Komagataella phaffii*, while
88 the strain of Guilliermond (CBS 704 or NRRL Y-1603) was regarded as the type strain of the
89 species *Komagataella pastoris*.

90 By the 1970's, these yeast species that can utilize methanol as the sole carbon source¹²⁻¹⁴
91 sparked the interest of Phillips Petroleum Company, since they had a vast supply of cheap
92 methane gas (a by-product of their oil refinement process), which can be easily oxidized to
93 methanol by chemical oxidation. Hence, they explored the available methylotrophic yeast species
94 through procedures that are not in the public domain, and selected a *Pichia pastoris* to grow on
95 the synthesized methanol and produce a single cell protein source for animal feed using
96 fermentation. The application was patented in 1980 (with the earliest priority application on April
97 12th, 1979)¹⁵, which required the strain to be deposited once more in public culture collections and
98 it became known as NRRL Y-11430 and CBS 7435. Which exact strain was deposited, is not
99 described in the patent, nor available in the public domain. It was already assumed that it could
100 be either the isolate from Guillermond (NRRL Y-1603) or that of H. Phaff (NRRL Y-4290)
101 (GRN 737). However, recent efforts of genomic sequencing show that the genetic differences
102 between both lineages are large enough to conclude that the latter was used^{16,17}.
103 In the early 80's, Phillips Petroleum Company contracted with the Salk Institute
104 Biotechnology/Industrial Associates (SIBIA) to develop the organism for recombinant protein
105 production, based primarily on the extremely strong and tightly regulated Alcohol Oxidase 1
106 promoter (pAOX1). In this context, NRRL Y-11430 derived strains were generated with
107 auxotrophies, such as the GS115 strain, which is a *his4* auxotrophic mutant obtained through
108 nitrosoguanidine mutagenesis of NRRL-Y11430¹⁸, and the X33 strain that is a *HIS4*
109 complemented strain deriving from GS115, likely via an intermediate¹⁸⁻²⁰. In 1993, Phillips
110 Petroleum sold its patent position in the *Pichia* system to Research Corporation Technologies
111 (RCT, Tucson, AZ)²¹, apparently including the strain patent deposits associated to this, and their
112 derived strains. Unfortunately, NRRL Y-11430 is not distributed anymore, likely because the
113 patentee is no longer under an obligation to provide the strain, given that the associated patent(s)
114 have expired almost 20 years ago. Indeed, the NRRL Y-11430 in the Agricultural Research
115 Service culture collection (ARS-NRRL) is no longer available, and the same is the case for the
116 CBS 7435 strain in the collection of the Westerdijk Fungal Biodiversity Institute (CBS). Also, it
117 appears that the strain and its popular derivatives, incl. their distribution, are still controlled by the
118 original patent holder. This occurs through the enforcement of Material Transfer Agreements
119 (MTAs) that were associated to obtaining the strain from the NRRL culture collection during the
120 time it was maintained as a patent deposit, or conditions of sale associated to obtaining derivative
121 strains through the commercial distribution by Invitrogen (currently a brand of Thermo Fisher
122 Scientific) as part of *Pichia* expression system kits. To our knowledge, the NRRL Y-11430
123 parental industrial strain can currently only be obtained at the American Type Culture Collection
124 (ATCC 76273) under a similarly restrictive MTA. Because of the RCT-mandated distribution of
125 *Pichia* expression technology kits by Invitrogen, for more than two decades, thousands of protein

126 expression labs have extensive experience with the GS115 family of strains that were included in
127 these kits^{22,23} and the currently approved biopharmaceuticals are manufactured by use of the
128 NRRL Y-11430 industrialized strain lineage. Many researchers are not fully aware of the
129 restrictions to strain distribution and potential applied use downstream of discoveries and
130 inventions made with them. Without prejudicing the legal aspects of some of this, which is outside
131 of our field of competence, as scientists we find it entirely unsatisfactory that the very basis of a
132 critical mainstay of academic and industrial biotechnology remains not simply openly accessible
133 exceedingly long after the original patents have expired. Given that *Pichia* takes such an ever
134 more prominent place in the toolkit for diverse sectors of synthetic biology and biotechnology, we
135 believe that it is long overdue for an open-access alternative strain platform to be set up by the
136 community. To continue to take benefit of the extensive regulatory agency acquaintance with
137 *Pichia*, it is important to achieve this by use of the same parental strain lineage as used in the
138 strains that were industrialized so far.

139 To achieve this goal, we and others have recently turned to the *Komagataella phaffii* type strains
140 that are present in culture collections throughout the world, armed with now highly affordable
141 genome resequencing, to try and identify the original isolate from nature that the Phillips
142 Petroleum researchers used in their derivation of NRRL Y-11430. In an exploration in the largest
143 US yeast strain collection (ARS-NRRL), the Love lab at MIT found that two deposits indicated by
144 the culture collection as equivalent *Komagataella phaffii* type strains (NRRL YB-4290, directly
145 deposited by Herman Phaff, and NRRL Y-7556), are genetically identical. Furthermore, in
146 comparison to this type strain, in their analysis they found only 1 point mutation leading to a
147 truncation of the Rsf2p open reading frame in NRRL Y-11430²⁴, establishing the type strain
148 lineage of this industrial strain. In this study, the NRRL type strains were found to have problems
149 with easily generating high copy number transformants and the authors recommended to keep
150 using the industrial NRRL Y-11430 strain background for recombinant protein production,
151 especially for expressions under methanol control. The NRRL YB-4290 strain is also present in
152 the UC Davis Phaff Yeast Culture Collection as its deposit made by Herman Phaff in 1954, and
153 numbered 54-11.239 (referred to as UCD-FST K-239 in the NRRL entries). It is documented in
154 the collections as having been isolated at Mather, Central Sierra Nevada, California, USA, from
155 the exudate flux of a black oak (*Quercus kelloggii*). Given its origin, no Access and Benefit Sharing
156 restrictions apply to its use for any purpose (Nagoya Protocol or Convention on Biological
157 Diversity). This type strain was also deposited in European culture collections: at the Westerdijk
158 Fungal Biodiversity Institute (CBS, Delft, The Netherlands, deposit CBS 2612) and at the National
159 Collection of Yeast Cultures (Norwich, UK, deposit NCYC 2543). In our present study, we started
160 out by analysing the genome of the four type strains. We then focused on the NCYC 2543 strain,
161 as the NCYC collection uniquely provides standard very affordable distribution and commercial

162 use licenses for its strains and derivatives thereof, fulfilling our requirements for a community
163 open-access *Pichia* platform strain. Different from all other culture collections where the *K. phaffii*
164 type strain deposits are found, technology developers can acquire a distribution license to end-
165 users for their newly generated materials, or have the choice of also depositing these in the NCYC
166 collection for full open access. Hence, we propose to nickname this NCYC 2543 type strain
167 deposit as 'OPENPichia'. In an effort to establish confidence in the OPENPichia strain as a new
168 standard open-access *Pichia* chassis for use by the research and biotechnological industry
169 community, we set out on a comprehensive characterization of its genome, growth characteristics,
170 transformation efficiency and recombinant protein expression, in comparison to the NRRL
171 Y-11430 industrial strain. We discovered a key frameshift mutation in the *HOC1* gene of the
172 industrial strain that enhances conduciveness to transformation, and introduced this mutation in
173 OPENPichia using open-source genome engineering technology, to overcome this important
174 limitation. Further characterization of this OPENPichia-*hoc1^{tr}* strain in comparison to NRRL
175 Y-11430 in terms of growth rate, cell wall density and cell sensitivity to cell envelope-binding
176 chemicals confirmed it to be indistinguishable phenotypically from the industrial strain. As set forth
177 below, we complement this OPENPichia strain set with an OPENPichia modular protein
178 expression vector toolkit, entirely made up of synthetic DNA to avoid any third-party MTAs, and
179 following the Golden Gate cloning standard for compatibility with complementary toolkits from
180 other *Pichia* developer labs²⁵. The basic NCYC 2543 OPENPichia strain is available from NCYC,
181 incl. straightforward and low-cost distribution licenses for labs that develop novel strains. Our own
182 derived OPENPichia strains described in this paper are openly available for end-users (incl. for
183 royalty-free *Pichia*-made commercial product manufacturing) under such distribution license that
184 our not-for-profit research institution VIB obtained from NCYC. OPENPichia vector cloning
185 materials are openly distributed for any utilization purpose in association with the public plasmid
186 collection of the Belgian Coordinated Collection of Microorganisms.

187

188 Results

189 The genomes of the *K. phaffii* type strains and commercial strains are virtually identical

190 To evaluate alternative *K. phaffii* strains at the genomic level, we deeply (avg. 180x genome
191 coverage) resequenced the genome of several type strains available at culture collections (i.e.,
192 NRRL YB-4290 / NRRL Y-7556 / CBS 2612 / NCYC 2543) in comparison to the NRRL Y-11430
193 industrial strain (**Error! Reference source not found.**) (Supplementary Table 1 and 2). The reads
194 were mapped against the published reference genome of the CBS 7435 strain incl. the
195 mitochondrial genome sequence and that of the two *K. phaffii* linear killer plasmids²⁶. CBS 7435
196 is a deposit of the NRRL Y-11430 industrial strain in the CBS culture collection (Delft, The

197 Netherlands). To this end, the Breseq²⁷ software package was used in consensus mode. There
198 was some variation in overall GC content, which can be attributed to the varying amount of
199 mitochondrial DNA and the presence of the two killer plasmids in some of the strains, as these
200 have an average GC content of 24%, 28% and 29%, respectively (unlike the nuclear
201 chromosomes, which have an average GC content of 41%). Indeed, the read alignment showed
202 that the proportion of reads that mapped to the mitochondrial genome varied between 10 and
203 47%.

204 The proportion of reads originating from the two killer plasmids, varied between 0% and 9%
205 (Supplementary Table 2). The *K. phaffii* killer plasmids are linear autonomously replicating DNA
206 fragments of 9.5 kb and 13.1 kb¹⁹ that encode exotoxins that can kill other yeast cells^{17,19}. These
207 toxins may also be toxic to cells from the same species, in case these have lost resistance to the
208 toxin, and this phenomenon is therefore undesired in large scale culturing of yeast as it may
209 reduce the overall viability of the culture. To verify the presence of such killer plasmids in the
210 tested strains, their sequences, as reported by Sturmberger *et. al.*, were included in the reference
211 for the alignment of the reads²⁶. Surprisingly, the killer plasmids could not be detected in both the
212 CBS 2612 and NCYC 2543 strain, while such reads were abundant for the analysed NRRL strains
213 (NRRL YB-4290, Y-7556 and Y-11430) (Table 2). According to the strain history, the NRRL
214 YB-4290 and CBS 2612 strains were deposited by Phaff, while the NRRL Y-7556 strain was a
215 redeposit of CBS 2612 by D. Yarrow (CBS). Since the daughter strain (NRRL Y-7556), still has
216 these killer plasmids, the mother strain (CBS 2612) should have had them as well, leading to the
217 conclusion that these linear plasmids are easily lost while propagating *K. phaffii* strains. In our lab
218 as well, several NRRL Y-11430 descendants were identified that have lost these killer plasmids
219 upon the standard microbial practice of single colony streaking (unpublished data). Also, the
220 commercial strain GS115, does not have any killer plasmids¹⁸.

221 Using a Maximum Likelihood method and the Hasegawa-Kishino-Yano model, a phylogenetic
222 tree based on the nuclear genome was computed to visualize the genetic distances between the
223 sequenced strains and a variety of other *K. phaffii* strains whose genomes were published
224 previously^{18,24,28}. All *K. phaffii* type strains are strongly clustered together with the NRRL Y-11430
225 and CBS 7435 strains, as well as other close relatives (Figure 2). Thus, these data support
226 previous literature^{24,29}, where it was hypothesized that all these strains are derived from the same
227 isolate, originally isolated by Phaff²⁸.

228 Based on the resequencing data, we identified single nucleotide polymorphisms (SNPs) and short
229 insertion-deletions (indels) (Table 2). First comparing the mutation calling of strain NRRL Y-11430
230 with the reference genome of the equivalent-deposit CBS 7435 strain reference revealed only
231 one protein-coding difference in one hypothetical protein and about 20 intergenic/intronic/silent
232 exonic differences. All these alterations were also identified in the type strains, indicating that

233 these are likely to be considered as the wild type *K. phaffii* genotype and that the CBS 7435
234 reference genome was most likely miscalled at these sites. The same holds for two insertions that
235 were observed in each of the sequenced strains in a region annotated to encode for a hypothetical
236 papain-like cysteine protease. This region appears to have been difficult to sequence in previous
237 experiments, as also in the datasets associated with a previous type strain genome sequencing
238 study²⁴, we found only a few reads mapping to this area, which were accompanied by many
239 mutations, low quality bases (Phred scores of <28) and low overall mapping quality score (<20).
240 Note that the type strain deposits of the different culture collections also differ from one another
241 each at one other coding sequence-altering genomic position and a few non-coding ones, likely
242 reflecting drift due to background mutational rate during strain propagation (Table 2 and 3).
243 We then focused on the very few protein-coding alterations that consistently distinguish the
244 industrial strain NRRL Y-11430 from the equivalent type strain deposits NRRL YB-4290, NRRL
245 Y-7556, CBS 2612, and NCYC 2543. Three coding sequence altering mutations (in *SEF1*, *RSF2*,
246 and *HOC1*) were shared by all type strains but were absent in the NRRL Y-11430 strain. Our re-
247 analysis of the raw sequencing reads from a previous genome analysis of deposits NRRL
248 YB-4290 and NRRL Y-7556 confirmed the presence of these mutations and their absence in the
249 NRRL Y-11430 strain also based on these datasets²⁴. Data quality in the area of the *SEF1* and
250 *HOC1* mutation is rather poor in these earlier datasets, and the authors only detected the mutation
251 in *RSF2*²⁴. Since all three mutations are shared by the type strains, it must be concluded that they
252 represent the original state of *K. phaffii*, and that NRRL Y-11430 is actually the mutant strain at
253 these three loci.

254

255 **Three mutations in protein-coding regions in the NRRL Y-11430/CBS 7435 industrial strain 256 lineage vs. the type strain deposits**

257 *SEF1* encodes for a putative transcription factor (UniProt ID F2QV09) and the observed SNP
258 causes a S315C mutation in NRRL Y-11430 as compared to the type strains. *RSF2* encodes for
259 a transcription factor which is involved in methanol- and biotin-starvation (UniProt ID F2QW29).
260 The observed mutation is a SNP which causes the introduction of a stop codon (W748*) in NRRL
261 Y-11430, resulting in the deletion of 183 amino acids from the C-terminus of the protein. The non-
262 truncated Rsf2p which is found in the *K. phaffii* type strains, is very similar to its homolog in *S.*
263 *cerevisiae*³⁰, additionally indicating that this was the original genomic state, as previously
264 reported²⁴. *HOC1* (homolog of *OCH1*) encodes for an α-1,6-mannosyltransferase (UniProt ID
265 F2QVW2) involved in the synthesis of cell wall mannan and is part of the M-PolII complex³¹. Here,
266 the industrial strain NRRL Y-11430 has a single base pair deletion in a poly-A stretch (at bp 755
267 of the 1191 bp long coding sequence), as compared to the type strains. This causes a frameshift
268 and premature stop codon, resulting in a C-terminally truncated protein (274 versus 398 amino

269 acids), with the last 22 amino acids up to the new stop codon being different from the type strain
270 sequence. The indel in the homopolymer was confirmed by Sanger sequencing (data not shown).
271 In parallel to our work, the same mutation was identified by the lab of Kenneth Wolfe (UC Dublin),
272 as the phenotype-causative mutation for a quantitative trait locus (QTL) that yielded 2-3 fold
273 higher secretion of a reported beta-glucosidase (personal communication, publication in press²⁹).
274 With this knowledge on which mutations could be involved in phenotypic differences between the
275 type strains and the industrial strains, we set out for a comparison of characteristics important to
276 the use of *Pichia* for recombinant protein production. Given that the NCYC 2543 deposit of the
277 type strain was the only one for which the resp. culture collection openly provides both commercial
278 and re-sale/strain distribution licenses as part of its standard business practice¹, we further mainly
279 focused on this deposit's characteristics, and we called it OPENPichia.
280

281 **Strain comparison for growth rate, protein production and transformation efficiency**

282 NCYC 2543/OPENPichia was compared to NRRL Y-11430 and GS115, both in terms of growth
283 rate and their capacity for expressing recombinant proteins. GS115 is a *his4* auxotrophic mutant
284 derived from NRRL Y-11430 by nitrosoguanidine mutagenesis and, depending on the analysis,
285 its genome contains about 69³², 74²⁴ or 71 (our unpublished data) mutations vs. that of its parent.
286 To be able to evaluated the impact of *his4*-mediated histidine auxotrophy on strain characteristics,
287 we generated an OPENPichia *his4* strain using the split-marker method^{33,34}. No significant
288 difference in growth rate between the type strains and NRRL Y-11430 could be observed
289 (**Error! Reference source not found.**), but the GS115 strain grew significantly more slowly (one-
290 way ANOVA, p=0.0034, Tukey test), as reported²⁴. Interestingly, our histidine auxotrophic
291 OPENPichia does not show the slower growth phenotype, demonstrating that this GS115
292 phenotype is not due to histidine auxotrophy, but rather must be due to one or more of the other
293 nitrosoguanidine-induced mutations in its genome. As *his4* complementation is an often-used
294 antibiotic-free selection marker, this unaffected growth rate in the OPENPichia *his4* strain is a
295 useful feature.
296

297 To compare the protein production capacity of the strains, a selection of model proteins was
298 produced in NRRL Y-11430 and OPENPichia (Table). Four proteins of very different types in use in biotechnology were chosen: a cytokine (GM-CSF), a redox enzyme (GaOx), a VHH-hFc α fusion (Cdiff-VHH-IgA), and a VHH-hFc γ fusion (CovidVHH-IgG). To enable recombinant expression, the two most commonly used off-patent *K. phaffii* promoters were tested: pGAP for strong constitutive and pAOX1 for strong methanol-inducible expression, respectively. Protein expression in *K. phaffii* is prone to clonal variations that can interfere with the comparison of expression capabilities between strains. Most of the

305 variation is due to the integration site and the copy number of the construct³⁵. To this end, a single-
306 copy was targeted to the respective promoter regions in the genome, the copy number and
307 integration site were confirmed by qPCR and integration-site specific PCR, and two independent
308 clones of each setup were grown in triplicate.

309 For both the pGAP-driven and pAOX1-driven expressions, there is in general no major difference
310 in protein production titres between the two hosts. However, there is a clear difference in cell
311 density at harvest of the pGAP cultures, with OPENPichia growing to higher densities than NRRL
312 Y-11430 (Supplementary Figure 1), whereas this is not the case on methanol. Additionally, in all
313 cases, NRRL Y-11430 shows slightly more host cell proteins (HCPs) in the medium of the pGAP
314 expressions (on limiting glucose), as visible on the SDS-PAGE gels (Figure 4), but not when
315 grown on methanol. Both observations point towards a minimally increased cell lysis of the NRRL
316 Y-11430 strain vs. the OPENPichia strain when grown on glucose.

317

318 ***HOC1*-truncation restores the transformation efficiency in NCYC 2543**

319 Upon generating expression clones, a strongly reduced transformation efficiency was observed
320 for OPENPichia as compared to NRRL Y-11430 (Figure 5C), as was also observed by others²⁴.
321 Out of the three consistent protein-coding differences between the type strains and NRRL
322 Y-11430, we reasoned that the one in the *HOC1* open reading frame could be causative for the
323 low transformation efficiency of the type strains, as the *S. cerevisiae* Hoc1p ortholog is an
324 α-1,6-mannosyltransferase that is part of the mannan polymerase II complex in the yeast Golgi
325 apparatus. The hypermannosyl-N-glycans, of which the backbone is synthesized by this mannan
326 polymerase complex, form the outermost layer of the ascomycete cell wall, and carry most of their
327 charge under the form of mannosylphosphate modifications on the side chains. *HOC1* deletion in
328 *S. cerevisiae* is viable though the phenotyping and genetic interaction data available in the
329 *Saccharomyces* Genome Database clearly indicate a cell wall stress response. As negatively
330 charged plasmid DNA during transformation has to traverse the cell wall, a cell wall that presents
331 less of a diffusional/charge barrier due to less mannan/mannosylphosphate density could explain
332 the more highly transformable phenotype of NRRL Y-11430. Using the split-marker method, we
333 introduced this single base pair deletion in the genome of OPENPichia, hence reverse
334 engineering the genetic makeup of the NRRL Y-11430 strain (Figure 5A) in this locus. Two mutant
335 versions were generated: NCYC 2543 *hoc1^{tr}-1*, where only the single base pair was deleted,
336 resulting in the truncated ORF and a Lox72-scar downstream of the novel stop codon; and NCYC
337 2543 *hoc1^{tr}-2*, where additionally 115 bp downstream of the novel stop codon were removed
338 (Figure 5B). The transformation efficiency was compared between the two wild type strains and
339 the *hoc1^{tr}* mutants, using a plasmid encoding for a VHH under control of the GAP or AOX1
340 promoter. The *HOC1*-truncation drastically increased the transformation efficiency of the

341 OPENPichia strain, and even showed a 2-3-fold improvement as compared to the NRRL Y-11430
342 in this experiment (Figure 5C). In general, it was also observed that the transformation efficiency
343 for pGAP-based plasmids is lower as compared to similar plasmids that are pAOX1-based, which
344 we speculate is due to the metabolic burden imposed by constitutive GBP VHH production during
345 recovery of the cells after transformation.

346

347 **Characterization of the NRRL Y-11430, NCYC 2543 and NCYC 2543 *hoc1^{tr}* cell wall**

348 These strains were further characterized in terms of their cell wall composition. First, the cell wall
349 mannoprotein N-glycans were profiled by capillary electrophoresis³⁶ after the cells were grown on
350 glucose or glycerol (Supplementary Figure 2). This method mainly detects the lower-degree of
351 polymerization N-glycans, and the profiles were very similar for all four strains, indicating that the
352 pathway of synthesis of the mannan core was intact in all strains. This capillary electrophoresis
353 method is however unsuited to the detailed profiling of the higher-polymerized mannan N-glycans,
354 as there are so many isomeric structures formed that are all in part or completely resolved, such
355 that they form one long trail of overlapping low-abundance peaks that is impossible to interpret.
356 Most of the mannosylphosphate negative charge-imparting moieties are added to the mannan
357 side branches of these long chains. They bind to cationic dyes such as Alcian Blue and hence
358 the staining density of yeast cells with such dye reflects the density of these negative charges on
359 the outermost layer of the cell wall. Indeed, as compared to the type strain NCYC
360 2543/OPENPichia, both NRRL Y-11430 and the two OPENPichia *hoc1^{tr}* mutants showed a
361 reduced Alcian Blue staining intensity (Figure 6A). This is consistent with the reduced Alcian Blue
362 staining of *S. cerevisiae* *hoc1* mutants^{37,38}.

363 To further investigate the cell wall integrity, resistance of the strains towards Congo red and
364 Calcofluor white was analysed (Figure 6B) using previously reported methods^{24,29}. The
365 OPENPichia type strain is much more resistant than NRRL Y-11430 towards both dyes, a
366 difference which is lost in the *HOC1*-truncated OPENPichia mutants. This indicates the
367 importance of Hoc1p in cell wall integrity. We also performed transmission electron microscopy
368 (TEM) using a freeze substitution technique that is optimized to pull in the osmium tetroxide
369 membrane-staining contrast reagent as well as fixatives through the cell wall during the slow
370 dehydration of the cells, which is then reversed in subsequent sample preparation. We observe
371 a much stronger electron scattering at the outermost cell wall layer of the wild type OPENPichia
372 type strain than for the other, *HOC1*-truncated strains (NRRL Y-11430 and OPENPichia *hoc1^{tr}*)
373 (Figure 6C). We interpret that this is caused by OsO₄-accumulation at the mannan layer of the
374 cell wall due to a stronger barrier to diffusion of the reagent in the wild type strain during freeze
375 substitution. Scanning electron microscopy looked very similar for the four strains (Figure 6C),
376 indicating no gross malformations. In summary, the data are consistent with the *hoc1^{tr}* mutation

377 resulting in a relatively mild cell wall integrity deficiency, resulting in increased passage of plasmid
378 DNA during transformation and, depending on the target protein, in some cases also increased
379 production or cell wall passage of secreted recombinant proteins²⁹.

380

381 **Strain comparison for growth rate and protein production of OPENPichia *hoc1^{tr}***

382 The growth rate, as well as protein production capacity of the newly generated OPENPichia
383 *HOC1*-truncated strains were compared to those of NRRL Y-11430 and wild type OPENPichia.
384 No significant difference in growth rate is observed between the 4 tested strains (Figure 7A). As
385 we earlier found most phenotypic difference between NRRL Y-11430 and wild type OPENPichia
386 in terms of growth and HCP levels when the strains were grown on glucose, we tested pGAP-
387 based protein expression for the different strains (Table 4), using an anti-GFP VHH (GBP) as test
388 protein. To this end, 24 clones of each strain were screened, except for wild type OPENPichia,
389 where only 12 transformants were obtained (Figure 7B and C). For pGAP-based GBP expression,
390 the NCYC 2543 *hoc1^{tr}* strains outperform the NCYC 2543 strain, and NCYC 2543 *hoc1^{tr}-1* even
391 outperforms NRRL Y-11430, although the differences are small and clonal distributions overlap.
392 The result is in line with the observations made by the Wolfe lab (personal communication,
393 publication in press²⁹), where they observed that the truncated *HOC1* genotype in NRRL Y-11430
394 resulted in doubling of the secretion level of a beta-glucosidase under control of the pGAP
395 promoter, vs. rather divergent *K. phaffii* NRRL strains.

396 The presented data together with the growth and expression analysis, show that the NCYC 2543
397 background is at least as good as an expression host as the industrial NRRL Y-11430 strain (or
398 its derivatives). With the discovery of the *HOC1* truncation as the basis for the higher
399 transformability of NRRL Y-11430, and the finding that it can easily be accomplished using free-
400 to-operate recombination-based genome engineering, also this last remaining handicap of the
401 parental NCYC 2543 was removed. Indeed, as reported recently by Brady *et al.*²⁴, the low
402 transformability, which makes it laborious to find clones with multicopy integration of the
403 expression vector, was the key reason for them to decide on continued use of NRRL Y-11430-
404 based strains over more wild type strains. This problem is now solved.

405 As no difference between the two NCYC 2543 *HOC1*-mutant versions could be observed and
406 given their excellent performance, we decided to continue all future *Pichia* work with the version
407 *hoc1^{tr}-1*, which has the smallest genomic scar downstream of the truncated *HOC1* coding
408 sequence (i.e., insertion of a remaining Lox72 site).

409

410 **OPENPichia modular protein expression vector construction toolkit**

411 Many scientists have used or still use commercial *K. phaffii* expression kits, which conveniently
412 match expression strains and vectors. Indeed, constraints in vector choice are sometimes

413 imposed by the properties of the chosen *K. phaffii* strain (e.g., selection markers, auxotrophies,
414 methanol utilization phenotypes, etc). Although such kits are attractive to beginner users and are
415 hence widespread within the scientific community, their conditions of sale are legally restrictive
416 and forbid further distribution and reutilization of vector parts, let alone use in commercial
417 production, which requires commercial licensing from the provider. Fortunately, issues with non-
418 FTO DNA constructs can nowadays be avoided by *de novo* synthesis, combined with novel and
419 fast cloning techniques which both emerged rapidly in the last decade³⁹. However, establishing a
420 new properly documented FTO genetic toolkit is still a relatively expensive and time-consuming
421 occupation for most labs.

422 To enable scientists to express their genes of interest, a well-equipped genetic toolkit and
423 corresponding cloning framework is provided to the community (Figure 8), and deposited at the
424 BCCM plasmid collection. The cloning system that was chosen is modular, to enable maximum
425 flexibility and based on Golden Gate cloning, similar to other toolkits^{25,40–48}. These cloning systems
426 have gained a lot of popularity as they are user-friendly and easily expandable, while also boasting
427 high versatility in construct design. In essence, the strength of Golden Gate assembly is based
428 on the use of Type IIS restriction endonucleases that cut outside their recognition sites, which
429 allows users to flank DNA fragments of interest with customizable 4 nt overhangs. As such, a
430 4 nt overhang of one fragment can be made complementary to a 4 nt overhang of another
431 fragment, and such compatible overhangs are ligated much more efficiently, enabling directional,
432 multi-insert cloning in a single reaction. The MoClo system takes this concept a step further, as it
433 standardizes Golden Gate assembly by designating *a priori* all DNA elements of a desired vector,
434 which are typically referred to as ‘parts’, to a particular ‘part type’ (e.g., promoter, CDS, etc) and
435 flanking each part type by unique 4 nt overhangs and Type IIS restriction sites⁴⁸. In practice, parts
436 are derived from PCR fragments or synthetic constructs, which are first subcloned in entry vectors,
437 also known as ‘Level 0’ vectors (Figure 8). As such, a collection of sequence-verified Level 0
438 vectors is established and vectors of interest can then be assembled into expression vectors of
439 interest, which are termed ‘Level 1’ vectors. By providing proper connector sequences with
440 additional Type IIS restriction sites, the resulting expression vectors or Level 1 vectors can then
441 be assembled again to obtain multigene or Level 2 vectors, which is the top level in the system’s
442 hierarchy. In the current toolkit, all 4 nt overhangs were adopted to ensure a high degree of
443 compatibility with existing yeast toolkits^{25,41,45} and to ensure a near 100% predicted ligation
444 fidelity⁴⁹. Since this toolkit is essentially derived from the *S. cerevisiae* MoClo system, it shares
445 the restriction enzymes (BsmBI and Bsal), most of the 4 nt overhangs, and the number and design
446 of the individual part types⁴¹. As such, the system is comprised of eight part types, of which
447 Part 3 (Coding Sequence) and Part 4 (Terminator) can still be split up to allow additional
448 modularity, for example to incorporate N- and C-terminal fusion partners for the protein of interest

449 (Figure 8). An overview of the part types and the parts that are provided in this OPENPichia toolkit
450 is included (Supplementary Figure 3). Part sequences are available in Supplementary Information
451 and materials can be obtained from the BCCM GeneCorner plasmid collection⁵⁰. The Material
452 Transfer Agreement associated with it was custom-designed in collaboration with GeneCorner to
453 allow for any use of resulting plasmids, including royalty-free commercial manufacturing.

454

455 Discussion

456 *Pichia pastoris* (formally known as *K. phaffii*) is an important protein production host in both
457 academia and industry, but the most common industrially developed strains are currently
458 distributed with restrictive MTAs, or not any longer. To facilitate academic and commercial host
459 strain development for recombinant protein expression and easy distribution throughout the
460 biotechnology community, alternative *K. phaffii* strains were investigated. We put forward an
461 open-access wild type strain, i.e., NCYC 2543 or OPENPichia, as well as two derivatives: a
462 histidine-auxotrophic strain and a *HOC1*-truncated strain with an improved transformation
463 efficiency. Moreover, a compatible genetic engineering toolkit is made available, which contains
464 all the necessary components for the expression of recombinant proteins and which can be easily
465 expanded with more genetic parts to fit the researcher's needs. This toolkit can be obtained with
466 an open-usage MTA from the GeneCorner plasmid collection, but it can also be assembled from
467 scratch, based on the sequences provided in the Supplementary Files 2.

468 It was shown that the proposed alternative OPENPichia strain (NCYC 2543) and its derivatives
469 are almost identical to the common NRRL Y-11430 strain. Only a handful of mutations could be
470 identified in our direct comparative genome analysis, of which only 4 are protein coding-altering
471 (SNPs and indels). Additionally, OPENPichia does not contain the undesired killer plasmids and
472 the strain shows the same maximum growth rate under the tested conditions. With respect to the
473 protein production capacity, the data presented here demonstrate that small differences can occur
474 between the *K. phaffii* type strain NCYC 2543/OPENPichia and NRRL Y-11430, but that there is
475 no consistently better performing strain, considering the variety of proteins tested in this study.
476 Previously, Brady et al²⁴, performed a similar experiment where NRRL Y-11430 showed to have
477 the highest protein expression level as compared to a series of other *K. phaffii* strains. However,
478 none of the type strains from which NRRL Y-11430 directly derives were included in this study;
479 instead, Y-12729 and Y-48124 (amongst others) were included, which are all members of Cluster
480 1 of their transcriptomics experiment. Y-7556 and YB-4290, which are type strains like NCYC
481 2543, are members of the transcriptomics Cluster 2, and would have allowed a better comparison.
482 Due to the increased cell wall robustness and reduced transformation efficiencies of the type
483 strains, they were excluded from the protein expression comparison in that study. Indeed, we also

484 observed that the transformation efficiency of the NCYC 2543 strain is dramatically lower as
485 compared to NRRL Y-11430. However, we could completely overcome this after our discovery
486 by more in-depth genome resequencing that NRRL Y-11430 has a truncating frameshift mutation
487 in the *HOC1* cell wall synthesis gene. We introduced the same frameshift mutations in *HOC1* of
488 OPENPichia, resulting in an even improved transformation efficiency as compared to NRRL
489 Y-11430. *Hoc1p* is part of one of two Golgi mannan polymerase complexes that in *S. cerevisiae*
490 also contains *Anp1p*, *Mnn9p*, *Mnn10p* and *Mnn11p*⁵¹, and which mediates elongation of the
491 α-1,6-mannan backbone that is initiated by the activity of *Och1p*. In *S. cerevisiae*, *HOC1* has
492 synthetic positive genetic interactions with the *PKC1* pathway that mediates responses to cell wall
493 stress, as well as genetic interactions with a multitude of genes involved in cell wall integrity,
494 protein secretion, vesicular transport, all key pathways in the yeast cell wall maintenance⁵².
495 Indeed, we observed a lower cell wall mannoprotein N-glycan mannosylphosphorylation density,
496 which is a sensitive hallmark of cell wall stress. The truncated *Hoc1p* that is produced in NRRL
497 Y-11430 vs. the type strain still has the alpha-helicoidal N-terminal luminal protein regions that
498 type II Golgi proteins typically use to space their catalytic domains away from the membrane, and
499 to interact with other Golgi proteins of similar topology. As *Hoc1p* forms part of such multi-protein
500 complex, we hypothesize that the truncated *Hoc1* allele maintains assembly of this complex but
501 lacks its own catalytic activity (see AlphaFold 2 model of the protein in Supplementary Figure 4).
502 In this way, likely a milder phenotype is obtained than with full *HOC1* deletion, making the *hoc1^{tr}*
503 strains grow equally well as the wild type.

504 Interestingly, under pGAP expression conditions, NRRL Y-11430 has somewhat more HCPs in
505 its culture supernatant and grows to a lower cell culture density as compared to OPENPichia. We
506 hypothesize that both observations are related and due to slightly increased cell lysis in NRRL
507 Y-11430, which can have an impact on the need for additional purification steps. Whether the
508 *hoc1^{tr}* mutation in OPENPichia has the same effect remains to be determined.

509 The *K. phaffii* strain that is proposed here as OPENPichia is one deposit of the type strain which
510 is widely available in many culture collections in different countries (see Global Catalogue of
511 Microorganisms)⁵³. For instance, strain CBS 2612 also does not have killer plasmids and is
512 identical but for a few drift mutations. If a *Pichia*-user is an end-user and wishes to merely
513 manufacture a product in these type strains, multiple culture collections provide cost-effective
514 licenses. However, for labs who are developing improved *Pichia* technology and implement these
515 novel inventions in the strains, strains have to be distributable to other laboratories, and this is
516 most often not allowed by the MTAs even of the public strain collections. NCYC should be
517 commended for uniquely transparently providing cost-effective resale/redistribution as well as

518 commercial manufacturing use licenses as part of standard culture collection practice, fulfilling an
519 essential need for yeast-based technology developers.

520 More broadly, our study illustrates the need to build 'generic' biotechnological platforms after
521 patents on these foundational inventions of our field expire, much in the same way as
522 'generic/biosimilar' medicines need to be developed to increase access to more affordable
523 medicines. We have previously also accomplished this for the HEK293 cell lineage that is used
524 for viral vector and vaccine manufacturing and hope that others will join us in such open science
525 endeavours for other synthetic biology 'chassis' systems⁵⁴. For now, we invite all *Pichia*
526 researchers and users to contribute to this OPENPichia resource and make best use of it.

527

528 **Materials & Methods**

529 **Strains and Media**

530 The wild type *K. phaffii* strains NRRL YB-4290, NRRL Y-7556 and NRRL Y-11430 were obtained
531 from the Agricultural Research Service (ARS, USA), CBS 2612 was obtained from Westerdijk
532 Institute (Netherlands) and NCYC 2543 was obtained from the National Collection of Yeast
533 Cultures (NCYC, UK). All mentioned strains were cultured and maintained on YPD or YPD agar.

534 All entry vectors and expression vectors were propagated and are available in the *E. coli* DH5 α
535 strain. MC1061 and MC1061 λ strains were used successfully as well and generally showed
536 higher transformation efficiency and easier green-white or red-white screening than was the case
537 for DH5 α . All *E. coli* strains were cultured and maintained on LB agar.

538 Antibiotics were used in the following concentrations for selection in *E. coli*: Zeocin 50 μ g/ml,
539 Nourseothricin 50 μ g/ml, Hygromycin 50 μ g/ml, Kanamycin 50 μ g/ml, Chloramphenicol 50 μ g/ml
540 and Carbenicillin 50 μ g/ml. Antibiotics were used in the following concentrations for selection in
541 *Pichia*: Zeocin 100 μ g/ml, Nourseothricin 100 μ g/ml, Hygromycin 100 μ g/ml, Geneticin 100 μ g/ml,
542 Blasticidin 100 μ g/ml.

543 Several media were used: LB (1% Tryptone, 0.5% Yeast Extract, 0.5% NaCl), YPD (1% Yeast
544 Extract, 2% Peptone, 2% D-glucose), YPG (1% Yeast Extract, 2% Peptone, 1% Glycerol), BMY
545 (1% Yeast Extract, 2% Peptone, 1,34% YNB without amino acids, 100 mM Potassium phosphate
546 buffer pH6), BMGY (BMY with 1% Glycerol), BMDY (BMY with 2% D-glucose), BMMY (BMY with
547 1% Methanol), and limiting glucose (1% Yeast Extract, 2% Peptone, 100mM Potassium
548 phosphate buffer pH6, 50g/l Enpresso EnPump substrate, 5ml/l Enpresso EnPump enzyme
549 solution (Enpresso GmbH, Germany)). For plates, 1.5% agar was added for LB media and 2%
550 for YPD media; when Zeocin selection was used, media were set to pH7.5.

551 All oligonucleotides and synthetic DNA fragments were ordered at Integrated DNA Technologies
552 (IDT), Leuven, Belgium. All synthetic DNA fragments (gBlocks® and Genes®) were designed and
553 adapted for synthesis using the Codon Optimization Tool and the gBlocks Gene Fragments Entry
554 Tool available at the website of IDT Europe.

555 **Illumina sequencing**

556 The strains were cultured overnight in YPD medium and the genomic DNA was extracted using
557 the Epicentre MasterPure™ Yeast DNA Purification Kit. Sample preparation (DNA fragmentation,
558 adapter ligation, size selection and amplification) and next generation sequencing (5M 150bp
559 paired end reads) was done by Eurofins, using Illumina technology. The reads were checked for
560 quality using fastqc⁵⁵, from which the %GC and number of reads was obtained. From the number
561 of reads, the average overall coverage was calculated with the formula

$$562 \frac{\# \text{reads} \times \text{read length (in bp)}}{\text{length of genomic DNA} + \text{mitochondrial DNA (in bp)}}.$$

563 **NGS analysis**

564 The reads were trimmed using Trimmomatic⁵⁶ to remove adapter, leading and trailing low quality
565 bases (cut off quality 3), low quality reads (4-base sliding window quality below 15) and reads
566 below 100 bp. Next, the reads were aligned to a reference and the mutations were identified using
567 Breseq²⁷ in consensus mode. As reference, the genome sequence published by Sturmberger *et*
568 *al.*²⁶ was used. The reference sequences for killer plasmids and the mitochondrial DNA were
569 obtained from Sturmberger *et. al.*²⁶ and Brady *et. al.*¹⁷, respectively. The reported coverage depth
570 was calculated by the Breseq algorithm. This is done by fitting a negative binomial distribution to
571 the read coverage depth observed at unique reference positions. The mean of this binomial fit is
572 used as the coverage depth. The killer plasmid copy number was estimated by comparing their
573 coverage depth with the average of the four chromosomes. The coverage depth for each molecule
574 was calculated as the mean of a binomial fit for the coverage depth for each reference position.

575 **Phylogenetic tree**

576 In order to make a phylogenetic tree, the sequencing data from this study was combined with the
577 raw reads that were published before²⁴ and also aligned as described above. From the predicted
578 mutations of both datasets, a whole genome alignment was constructed from which a
579 phylogenetic tree was calculated using the Mega X⁵⁷ software package. A maximum likelihood
580 algorithm was used with an HKY substitution matrix.

581 **Creation of the NCYC2543 *his4* strain**

582 The NCYC2543 *his4* strain was generated using the split-marker method that was described
583 previously by Heiss *et al.*⁵⁸. The homology arms of the *HIS4* gene were selected from Näätsaari

584 *et al.*⁵⁹, and the reference genome of the CBS7435 strain. First, a construct containing the two
585 homology arms with a floxed Nourseothricin acetyltransferase marker was created. Next two
586 overlapping fragments containing one of the homologies and a part of the antibiotic marker were
587 generated by PCR using Taq polymerase (Promega), which overlap for a length of 594 bp. These
588 fragments were purified by a phenol chloroform precipitation. In brief, after adding an equal
589 volume of phenol:chloroform:isoamyl alcohol (25:24:1), the solution was mixed, centrifuged
590 (5 min at 12,000 g) and the liquid phase was isolated by decanting. To this, 1/10th volume of 3 M
591 sodium acetate pH 5.5 and 2 volumes of 100% ethanol was added and the sample was mixed
592 and centrifuged (15 min at 12,000 g). Afterwards, the pellet, containing the amplified DNA, was
593 isolated, washed with 70% ethanol, air-dried, and resuspended in water.

594 Both purified fragments were transformed into NCYC 2543 competent cells by electroporation
595 and transformants were streaked to single clone onto YPD plates containing Nourseothricin and
596 grown for 2 days at room temperature. The resulting clones were replica plated onto CSM-his
597 plates for growth screening and grown for 2 days at room temperature. Strict non-growers were
598 checked by colony PCR for replacement of the *HIS4* gene with the antibiotic marker cassette.

599 The Nourseothricin acetyltransferase marker was finally removed by transient expression of a
600 Cre-recombinase. This gene was cloned into a plasmid with an ARS⁶⁰ and a Zeocin resistance
601 cassette, which was then transformed in the *his4* strain. Transformants were incubated overnight
602 on a YPD plate containing Zeocin and colonies were transferred to YPD plates without antibiotics.
603 The removal of the antibiotic cassettes of the plasmid and *HIS4* knock-out was verified with replica
604 plating on YPD containing the respective antibiotics and double-checked via colony PCR.

605 **Creation of the NCYC2543 *hoc1^{tr}* strains**

606 The NCYC2543 *hoc1^{tr}* strains were generated using the split-marker method as described above.
607 The left homology arm of the *HOC1* gene was chosen such as to contain about 1 kb upstream of
608 the premature stop codon. To introduce the single nucleotide deletion, genomic DNA of NRRL
609 Y-11430 instead of NCYC 2543 was used as the PCR template. The right homology arm was
610 chosen as to contain about 1 kb downstream of the premature stop codon, also for this PCR,
611 genomic DNA of NRRL Y-11430 was used, although NCYC 2543 would have also worked. The
612 left and right homology arms were respectively fused by PCR to the first and last two thirds of the
613 floxed Nourseothricin acetyltransferase marker. The PCR fragments were purified over gel and
614 the DNA was recovered using the Wizard SV Gel and PCR Clean-Up System (Promega),
615 according to the manufacturer's instructions. Both purified fragments were transformed into NCYC
616 2543 competent cells by electroporation and transformants were streaked to single clone onto
617 YPD plates containing Nourseothricin and grown for 2 days at room temperature. The resulting
618 clones were screened using colony PCR using a forward primer annealing upstream of the left

619 homology arm and a reverse primer annealing to the Nourseothricin selection marker. The
620 Nourseothricin acetyltransferase marker was removed by transient expression of a Cre-
621 recombinase as described above. The engineered *HOC1* locus was confirmed for both strategies
622 by colony PCR and Sanger sequencing. The sequences for the PCR primers and split-marker
623 cassettes can be found in Supplementary Tables 3 and 4.

624 **Growth Analysis**

625 The different *Pichia* strains were cultured on YPD agar for 2 days, inoculated in triplicate into a
626 5 ml preculture of BMDY and grown overnight at 28 °C, shaking at 225 rpm. The optical density
627 at 600 nm (OD₆₀₀) of each culture was measured and 250 ml of BMDY was inoculated at a starting
628 OD₆₀₀ of 0.05. Samples of 1 ml were immediately isolated from each culture to measure the OD₆₀₀
629 again. Then, samples of 1 ml were isolated every 2 h for 22 hours and again after 26 hours and
630 29 hours. All samples were diluted accordingly and measured within an OD₆₀₀ range of 0.05 – 1.

631 **Recombinant protein expressions**

632 The expression vectors were made using the MoClo toolkit, based on Golden Gate cloning as
633 described in this paper. Briefly, the protein coding sequences were ordered synthetically with Part
634 3b type Bsal overhangs (NEB R3733) and cloned into the entry vector with BsmBI (NEB R0739).
635 Next, expression vectors were made by assembly of the Level 0 parts.

636 The cloning procedure was as follows: 1 µl of T4 DNA Ligase (400 U; NEB M0202), 2 µl of T4
637 DNA Ligase Buffer (NEB M0202), 1 µl of Restriction Enzyme (20 U) were added to 20 fmoles of
638 backbone (pPTK081 for entry vectors; any P8 backbone for destination vectors). An excess of
639 insert (>1000 fmoles of PCR amplicon or synthetic gene; 10 pmoles of annealed oligonucleotides)
640 was added for a BsmBI assembly, while equimolar amounts (20 fmoles) of each entry vector were
641 added for a Bsal assembly. BsmBI assembly mixtures were incubated according to the following
642 protocol: >25 cycles of 42 °C for 2 min (digest) and 16 °C for 5 min (ligation), followed by 60 °C
643 for 10 min (final digest) and 80 °C for 10 min (heat inactivation step). Bsal assembly mixtures
644 were incubated similarly, except that the digestion steps were performed at 37 °C.

645 *Pichia* electrocompetent cells were generated, using the lithium acetate method as described by
646 Wu *et al.*⁶¹. In brief, precultures were inoculated in 5 ml YPD and grown overnight in an incubator
647 at 28 °C and 250 rpm. The precultures were diluted and grown to an OD₆₀₀ of approximately 1.5.
648 50 ml of the culture was isolated and the cells were harvested by centrifugation (1,519 g for 5 min
649 at 4 °C), resuspended in 200 ml of a lithium acetate (LiAc)/dithiothreitol (DTT) solution (100 mM
650 LiAc, 10 mM DTT, 0.6 M sorbitol, 10 mM Tris-HCl pH 7.5) and incubated for 30 minutes at 28 °C
651 and 100 rpm. Next, the cells were collected by centrifugation (1,519 g for 5 min at 4 °C), washed
652 two times with 1 M ice-cold sorbitol and finally resuspended in 1.875 ml of 1 M ice-cold sorbitol.

653 0.5 to 1 µg of DNA was added to aliquots of 80 µl and electroshocked (1.5kV, 200Ω, 25µF).
654 Immediately, 1 ml of 1 M sorbitol was added and the suspension was incubated at 28 °C for
655 2-5 h. Next, the cells were plated on YPD agar containing the appropriate antibiotic, and colonies
656 were isolated after 2 days of incubation at 30 °C.

657 To be able to compare expression, only colonies with single copy integration of the construct were
658 selected. The copy number was determined by quantitative PCR on a Lightcycler 480 (Roche)
659 using primers that bind pAOX1 and pGAP. The genes *OCH1* and *ALG9* were used as reference.
660 Genomic DNA (gDNA) of NCYC 2543 was included as a single copy positive control. A single
661 copy plasmid integration will yield one additional copy and more than two copies would be the
662 result of multiple plasmid integrations. Amplification efficiencies were determined using serial
663 dilutions of gDNA samples. Reactions were set up in 10 µl with final concentrations of 300 nM
664 forward primer, 300 nM reverse primer, 1x SensiFast SYBR no-rox mastermix (Bioline), 10 ng
665 gDNA and the following cycling conditions: 3 min at 95 °C, followed by 45 cycles of 95 °C for 3 s,
666 60 °C for 30 s at ramp rate 2.5 °C/s, 72 °C for 1 s, ending with 0.11 °C/s from 65 °C to 95 °C for
667 melting curve determination (5 acquisitions/s). Copy numbers were calculated using the
668 ΔΔC_t method⁶².

669 The different strains expressing the recombinant proteins, were cultured on YPD agar plates for
670 2 days, inoculated in triplicate into a 5 ml preculture of BMDY and grown overnight at 28 °C,
671 shaking at 225 rpm. Next, the cultures for pAOX1-driven expression, were inoculated in BMDY,
672 grown for 24 h, subsequently transferred to BMMY and incubated for 48 h. After 24 h in BMMY,
673 an extra 1% of methanol was added. The cultures for pGAP-driven expression, were instead
674 inoculated in limiting glucose medium and incubated for 48 h. Then, optical density at 600nm was
675 measured for all cultures and the supernatant was collected by centrifuging (2,500 g for 5 min).
676 The samples were incubated with EndoH (produced in-house) to remove N-glycans and analysed
677 by SDS-PAGE.

678 **ELISA-based quantification of GBP**

679 Nunc MaxiSorp™ 96-well plates were coated with 75 ng/well of penta-His antibody in PBS
680 solution (Qiagen, 34660) and incubated overnight at 4 °C. Plates were washed three times with
681 200 µl/well of wash buffer (PBS + 0.05% Tween-20) and any residual liquid was removed. Plates
682 were blocked with 100 µl/well Reagent Diluent (1% Probumin (Millipore, 82-045-1) in PBS pH 7.2)
683 for 2 h. Plates were washed three times with 200 µl/well of wash buffer and residual liquid was
684 removed. Dilutions of the yeast supernatant were prepared in 96-deepwell plates and 100 µl of a
685 100,000-fold dilution was applied to the plates and incubated for 1 hour while shaking gently on
686 a table top plate shaker. Plates were washed three times with 200 µl/well of wash buffer and
687 residual liquid was removed. Plates were provided with 100 µl of a 250 ng/ml MonoRab™ Rabbit

688 Anti-Camelid VHH Antibody coupled to HRP in Reagent Diluent and incubated for 1 hour while
689 shaking gently on a table top plate shaker. Plates were washed three times with 200 μ l/well of
690 wash buffer and residual liquid was removed. TMB substrate was prepared according to the
691 manufacturer's instructions (BD OptEIATM) and 100 μ l/well was applied to the plate before
692 incubating for 10 min. Next, 50 μ l of stop solution (2N H₂SO₄) was added to each well and the
693 plate was read at 450 nm by a plate reader. Absorbance units were background corrected. All
694 strains were compared in a Kruskal-Wallis omnibus test, followed by pairwise comparison
695 corrected with Dunn's multiple comparison procedure.

696 **Transformation efficiency testing**

697 Competent cells were prepared using the lithium acetate method as described above. 200 ng of
698 linearized plasmid was transformed to each strain and several dilutions of the transformation mix
699 were plated on either non-selective YPD agar or YPD agar containing 100 μ g/ml Zeocin. For each
700 transformation, colonies were counted from the plates where clear individual colonies could be
701 observed after 2 days at 30 °C incubation. Both the selective and non-selective plates were
702 counted to correct for a potential difference in the number of competent cells per transformation.

703 A linear model (estimated using ordinary least squares) in the statistical software R was fitted⁶³.
704 As the outcome variable, the log-transformed, normalized transformation efficiency (natural log of
705 the number of transformants per million clones) and as predictor variables the strain and promotor
706 type, including an interaction effect were used. The model explains a statistically significant and
707 substantial proportion of variance ($R^2=0.94$, $F(7,38)=81.33$, $p<.001$, adj. $R^2=0.93$). Model-
708 predicted group means with 95% confidence intervals were obtained using the ggeffects package
709 with heteroscedasticity-consistent variance estimators from the sandwich package (vcovHC, type
710 HC0)^{64,65}. Further, we defined specific contrasts using the multcomp package⁶⁶, again with
711 heteroscedasticity-consistent variance estimators to obtain multiple-comparison corrected
712 estimates for the ratios of transformation efficiencies between the different strains and using
713 different plasmids.

714 **DSA-FACE-based glycan analysis of the cell wall mannoproteins**

715 Strains were inoculated in YPD or YPG, from their respective precultures, at an OD₆₀₀ of 0.05 and
716 grown overnight at 28 °C and 200 rpm. The next day, 500 OD units per strain were pelleted
717 (10 min at 1,500 g) and the mannoproteins were isolated, as follows. The pellets were washed
718 three times with Milli-Q, after which 20 mM of citrate buffer pH6.6 was added at 1 ml per 150 μ g
719 of wet cell weight. The resuspended cells were autoclaved for 1.5 hours at 120 °C in cryovials
720 and then centrifuged for 10 min at 16,000 g. To the supernatant fractions, 3 volumes of ice-cold
721 methanol were added and the vials were incubated for 15 min at 20 °C. The mannoproteins were

722 spun down for 10 min at 16,000 g and the pellets were left to dry until transparent. The pellets
723 were resuspended in 50 μ l RCM buffer (8 M Urea, 360 mM Tris-HCl pH 8.6, 3.2 mM EDTA) and
724 stored at 4 °C until further analysis.

725 The N-linked oligosaccharides were prepared from the purified mannoproteins upon blotting to
726 PVDF membrane in the wells of 96-well plate membrane plates, and were analysed by capillary
727 electrophoresis with laser-induced fluorescence detection (CE-LIF) using an ABI 3130 capillary
728 DNA sequencer as described previously³⁶.

729 **Alcian blue assay**

730 The assay was performed as described previously³⁷, with adaptations. Briefly, Alcian blue was
731 prepared in 0.02 N HCl at a concentration of 63 μ g/ml and the solution was centrifuged to remove
732 insoluble precipitates. An overnight culture of each strain was grown in YPD at 28 °C and
733 200 rpm. The next day, the cells were pelleted and the supernatant was removed. The cells were
734 washed with 0.02 N HCl and the pellet was resuspended again in 0.02 N HCl to an OD₆₀₀ of
735 10 OD/ml. 100 μ l (1 OD₆₀₀) of cells was transferred to a 96-V-bottom plate to which 100 μ l of the
736 Alcian blue solution was added. After 15 min of incubation at room temperature, the plate was
737 centrifuged for 15 min at 3,220 g, after which the pellets were visually checked.

738 **Congo red and Calcofluor white test**

739 The test was performed as described elsewhere⁶⁷, with slight adaptations. Briefly, the strains were
740 grown overnight in BMGY. The next day, dilutions were made in order to obtain 10E5 to 10E1
741 cells in 5 μ l BMGY. 5 μ l drops were spotted on the different plates and the plates were incubated
742 for 3 days at 30 °C. Congo red (Sigma, C6767) and Calcofluor white (Fluka, 18909) were present
743 at final concentrations of 75 μ g/ml and 10 μ g/ml, respectively.

744 **Electron microscopy**

745 *Transmission electron microscopy*

746 The strains were cultivated in BMGY at 28 °C and 200 rpm, overnight. High Pressure Freezing,
747 as described previously⁶⁸, was carried out in a high-pressure freezer (Leica EM ICE; Leica
748 Microsystems, Vienna, Austria). Cells were pelleted and frozen as a paste in 150 μ m copper
749 carriers. HPF was followed by Quick Freeze Substitution as described previously⁶⁹. Briefly,
750 carriers were placed on top of the frozen FS solution inside a cryovial containing 1% ddH₂O,
751 1% OsO₄ and 0.5% glutaraldehyde in dried acetone. After reaching 4 °C for 30 min, samples were
752 infiltrated stepwise over three days at 0-4 °C in Spurr's resin and embedded in capsules. The
753 polymerization was performed at 70 °C for 16 h. Ultrathin sections of a gold interference colour

754 were cut using an ultra-microtome (Leica EM UC6), followed by a post-staining in a Leica EM
755 AC20 for 40 min in uranyl acetate at 20 °C and for 10 min in lead stain at 20 °C.
756 Sections were collected on formvar-coated copper slot grids. Grids were viewed with a JEM-
757 1400Plus transmission electron microscope (JEOL, Tokyo, Japan) operating at 60 kV.

758 *Scanning electron microscopy*

759 The strains were cultivated in BMGY at 28 °C and 200 rpm, overnight. Cells were fixed overnight
760 in 1.5% Paraformaldehyde, 3% Glutaraldehyde in 0.05 M Na-Cacodylate buffer pH7.4. The fixed
761 cells were centrifuged for 2 min at 1,000 g between each following step. First the cells were
762 washed 3 times with 0.1 M Na-Cacodylate buffer pH7.4 and then incubated for 30 min in 2% OsO₄
763 in 0.1 M Na-Cacodylate pH7.4. Osmicated samples were washed 3 times with Milli-Q, prior to a
764 stepwise ethanol dehydration (50%, 70%, 90%, 2 x 100%). Samples were incubated twice in
765 hexamethyldisilazane (HMDS) solution (Sigma-Aldrich), as a final dehydration step, after which
766 they were spotted on silicon grids (Ted Pella) and air-dried overnight at room temperature.
767 Samples were next coated with 5 nm Platinum (Pt) in a Quorum Q 150T ES sputter coater
768 (Quorum Technologies) and placed in a Gemini 2 Cross beam 540 microscope from Zeiss for
769 SEM imaging at 1.50 kV using a SE2 detector.

770

771 **Associated content**

- 772 • All plasmids from the modular cloning kit are available at the Belgian Co-ordinated
773 Collections of Micro-organisms (BCCM)/GeneCorner Plasmid Collection
774 (<http://bccm.belspo.be/about-us/bccm-genecorner>).
- 775 • All raw reads of the genomes sequenced in this study have been submitted to NCBI and
776 can be found under the following accession numbers: NRRL Y-11430 (SAMN32067769),
777 NRRL YB-4290 (SAMN32067770), NRRL Y-7556 (SAMN32067773), NCYC 2543
778 (SAMN32067771), CBS 2612 (SAMN32067772).
- 779 • Supplementary Figure 1: Summary of the end-ODs of the pGAP- and pAOX1-based
780 cultivations at harvest.
- 781 • Supplementary Figure 2: DSA-FACE profiles of the cell wall mannoproteins of the different
782 strains grown on YPD or YPG.
- 783 • Supplementary Figure 3: Overview of the available elements for the different parts of the
784 MoClo toolbox.
- 785 • Supplementary Figure 4: AlphaFold 2 models of the type strain Hoc1p and of the NRRL
786 Y-11430 lineage derived strain.

787 • Supplementary Table 1: Overview of the NGS results, including the number of reads, GC%
788 and average overall coverage.

789 • Supplementary Table 2: Proportion of NGS reads mapping to different molecules of the
790 reference genome, mitochondrial DNA and killer plasmids.

791 • Supplementary Table 3: List of oligonucleotides that were used as primers for PCR, cPCR
792 or sequencing.

793 • Supplementary Table 4. Sequences of the split-marker fragments used to generate the two
794 *HOC1* mutants.

795 • Supplementary File 1: GenBank files of the expression constructs used in the study.

796 • Supplementary File 2: FASTA files of the available MoClo Parts.

797

798 **Author Information**

799 This work was originally conceived and initiated by DVH, KV and NC. DVH, RV, KV, SV, EW,
800 BVM, HE, DF, HG, CL, GM, LM, JN, CR, LVS, and KC performed experiments and contributed
801 to data analysis and/or results presentation. RDR, MDB and PB performed the electron
802 microscopy. DVH, RV, KC and NC cowrote the manuscript, while KC and NC supervised the
803 work.

804

805 **Acknowledgements**

806 DVH was supported by a Baekeland mandate of VLAIO (Flanders Innovation & Entrepreneurship
807 fund) in collaboration with Inbiose NV, and is now an employee of Inbiose NV. RV was supported
808 by a Strategic Basic Research fellowship from the Fund for Scientific Research and otherwise
809 supported by Ghent University and is now an employee of Those Vegan Cowboys. KV was a VIB
810 post-doctoral fellow and is now employee of Inbiose NV. SV and EW are employees of the Ghent
811 University. HE is supported by a Fundamental Research fellowship of the Fund for Scientific
812 Research Flanders (FWO). HG was a post-doctoral fellow funded by the Ghent University and
813 VIB and is now an employee of Eurofins. CL was supported by a Strategic Basic Research
814 fellowship of the Fund for Scientific Research Flanders (FWO) and is now an employee of Exevir.
815 LM and DF are staff scientists of the VIB Center for Medical Biotechnology. GM was supported
816 by VIB and now works at Animab. JN, CR and BVM are supported by Strategic Basic Research
817 fellowships of the Fund for Scientific Research Flanders (FWO). LVS is a VIB post-doctoral fellow
818 and supported by grants from the Industrial Research Fund of Ghent University, VLAIO and the
819 European Commission (HERA-Pilot). RDR, MDB and PB are employees of VIB. KC is supported
820 by an Innovation Mandate of VLAIO. Research in the Callewaert lab is supported by grants from

821 UGent, the Fund for Scientific Research Flanders (FWO) and core resources from VIB. We want
822 to thank Joeri Beauprez for valuable discussions; and Erhan Çitak, Merve Arslan, Annelies Van
823 Hecke and Simon Devos for assistance with some of the experiments.

824

825 **References**

- 826 1. Licences | National Collection of Yeast Cultures. <https://www.ncyc.co.uk/licences>.
- 827 2. Karbalaei, M., Rezaee, S. A. & Farsiani, H. *Pichia pastoris*: A highly successful expression
828 system for optimal synthesis of heterologous proteins. *J Cell Physiol* **jcp.29583** (2020)
829 doi:10.1002/jcp.29583.
- 830 3. Adivitiya, Dagar, V. K. & Khasa, Y. P. Yeast Expression Systems: Current Status and Future
831 Prospects. in *Yeast Diversity in Human Welfare* (eds. Satyanarayana, T. & Kunze, G.) 215–
832 250 (Springer Singapore, 2017). doi:10.1007/978-981-10-2621-8_9.
- 833 4. Yang, Z. & Zhang, Z. Engineering strategies for enhanced production of protein and bio-
834 products in *Pichia pastoris*: A review. *Biotechnology Advances* **36**, 182–195 (2018).
- 835 5. Baumschabl, M. *et al.* Conversion of CO₂ into organic acids by engineered autotrophic yeast.
836 *Proc Natl Acad Sci U S A* **119**, e2211827119 (2022).
- 837 6. Liu, L. *et al.* How to achieve high-level expression of microbial enzymes: strategies and
838 perspectives. *Bioengineered* **4**, 212–223 (2013).
- 839 7. Gasser, B. *et al.* *Pichia pastoris*: protein production host and model organism for biomedical
840 research. *Future Microbiology* **8**, 191–208 (2013).
- 841 8. Phaff, H. J., Miller, M. W. & Shifrine, M. The taxonomy of yeasts isolated from *Drosophila* in
842 the Yosemite region of California. *Antonie van Leeuwenhoek* **22**, 145–161 (1956).
- 843 9. Phaff, H. J. A proposal for amendment of the diagnosis of the genus *Pichia* hansen. *Antonie van Leeuwenhoek* **22**, 113–116 (1956).
- 844 10. Yamada, Y., Matsuda, M., Maeda, K. & Mikata, K. The Phylogenetic Relationships of
845 Methanol-assimilating Yeasts Based on the Partial Sequences of 18S and 26S Ribosomal
846 RNAs: The Proposal of *Komagataella* Gen. Nov. (Saccharomycetaceae). *Bioscience, Biotechnology, and Biochemistry* **59**, 439–444 (1995).
- 847 11. Kurtzman, C. P. Description of *Komagataella phaffii* sp. nov. and the transfer of *Pichia*
848 pseudopastoris to the methylotrophic yeast genus *Komagataella*. *INTERNATIONAL
849 JOURNAL OF SYSTEMATIC AND EVOLUTIONARY MICROBIOLOGY* **55**, 973–976 (2005).
- 850 12. Ogata, K., Nishikawa, H. & Ohsugi, M. A yeast capable of utilizing methanol. *Agricultural and
851 biological chemistry* **33**, 1519–1520 (1969).
- 852 13. Tani, Y., Miya, T., Nishikawa, H. & Ogata, K. The Microbial Metabolism of Methanol: Part I.
853 Formation and Crystallization of Methanol-oxidizing Enzyme in a Methanol-utilizing Yeast,
854 *Kloeckera* sp. No. 2201 Part II. Properties of Crystalline Alcohol Oxidase from *Kloeckera* sp.
855 No. 2201. *Agricultural and Biological Chemistry* **36**, 68–83 (1972).
- 856 14. TANI, Y., MIYA, T. & OGATA, K. The microbial metabolism of methanol Part II. *Agricultural
857 and Biological Chemistry* **36**, 76–83 (1972).
- 858 15. Wegner Eugene Herman. A Process For Producing Single Cell Protein Material And Culture.
859 (1980).
- 860 16. Kurtzman, C. P. Biotechnological strains of *Komagataella* (*Pichia*) *pastoris* are *Komagataella*
861 *phaffii* as determined from multigene sequence analysis. *J Ind Microbiol Biotechnol* **36**, 1435–
862 1438 (2009).
- 863 17. Love, K. R. *et al.* Comparative genomics and transcriptomics of *Pichia pastoris*. *BMC
864 genomics* **17**, 550 (2016).

867 18. De Schutter, K. *et al.* Genome sequence of the recombinant protein production host *Pichia*
868 *pastoris*. *Nature biotechnology* **27**, 561 (2009).

869 19. Sturmberger, L. *et al.* Refined *Pichia pastoris* reference genome sequence. *Journal of*
870 *biotechnology* **235**, 121–131 (2016).

871 20. Mattanovich, D. *et al.* Open access to sequence: browsing the *Pichia pastoris* genome.
872 *Microbial cell factories* **8**, 53 (2009).

873 21. *Pichia* Technology from RCT. <https://pichia.com/>.

874 22. Gasser, B. *et al.* *Pichia pastoris*: protein production host and model organism for biomedical
875 research. *Future Microbiology* **8**, 191–208 (2013).

876 23. Fischer, J. E. & Glieder, A. Current advances in engineering tools for *Pichia pastoris*. *Current*
877 *Opinion in Biotechnology* **59**, 175–181 (2019).

878 24. Brady, J. R. *et al.* Comparative genome-scale analysis of *Pichia pastoris* variants informs
879 selection of an optimal base strain. *Biotechnology and Bioengineering* **117**, 543–555 (2020).

880 25. Prielhofer, R. *et al.* GoldenPiCS: a Golden Gate-derived modular cloning system for applied
881 synthetic biology in the yeast *Pichia pastoris*. *BMC Syst Biol* **11**, 123 (2017).

882 26. Sturmberger, L. *et al.* Refined *Pichia pastoris* reference genome sequence. *Journal of*
883 *Biotechnology* **235**, 121–131 (2016).

884 27. Deatherage, D. E. & Barrick, J. E. Identification of Mutations in Laboratory-Evolved Microbes
885 from Next-Generation Sequencing Data Using breseq. in *Engineering and Analyzing*
886 *Multicellular Systems* (eds. Sun, L. & Shou, W.) vol. 1151 165–188 (Springer New York,
887 2014).

888 28. Braun-Galleani, S. *et al.* *Tetrad analysis without tetrad dissection: Meiotic recombination and*
889 *genomic diversity in the yeast Komagataella phaffii (Pichia pastoris)*. <http://biorxiv.org/lookup/doi/10.1101/704627> (2019) doi:10.1101/704627.

890 29. Offei, B. *et al.* Identification of genetic variants of the industrial yeast *Komagataella phaffii*
891 (*Pichia pastoris*) that contribute to increased yields of secreted heterologous proteins. *PLoS*
892 *Bio* **20**, (2022).

893 30. Lu, L., Roberts, G. G., Oszust, C. & Hudson, A. P. The YJR127C/ZMS1 gene product is
894 involved in glycerol-based respiratory growth of the yeast *Saccharomyces cerevisiae*. *Current*
895 *genetics* **48**, 235–246 (2005).

896 31. Jungmann, J. & Munro, S. Multi-protein complexes in the *cis* Golgi of *Saccharomyces*
897 *cerevisiae* with alpha-1,6-mannosyltransferase activity. *EMBO J* **17**, 423–434 (1998).

898 32. Braun-Galleani, S. *et al.* Genomic diversity and meiotic recombination among isolates of the
899 biotech yeast *Komagataella phaffii* (*Pichia pastoris*). *Microb Cell Fact* **18**, 211 (2019).

900 33. Fairhead, C., Llorente, B., Denis, F., Soler, M. & Dujon, B. New vectors for combinatorial
901 deletions in yeast chromosomes and for gap-repair cloning using 'split-marker'recombination.
902 *Yeast* **12**, 1439–1457 (1996).

903 34. Heiss, S., Maurer, M., Hahn, R., Mattanovich, D. & Gasser, B. Identification and deletion of
904 the major secreted protein of *Pichia pastoris*. *Appl Microbiol Biotechnol* **97**, 1241–1249
905 (2013).

906 35. Vogl, T., Gebbie, L., Palfreyman, R. W. & Speight, R. Effect of Plasmid Design and Type of
907 Integration Event on Recombinant Protein Expression in *Pichia pastoris*. *Appl Environ*
908 *Microbiol* **84**, e02712-17, /aem/84/6/e02712-17.atom (2018).

909 36. Laroy, W., Contreras, R. & Callewaert, N. Glycome mapping on DNA sequencing equipment.
910 *Nat Protoc* **1**, 397–405 (2006).

911 37. Conde, R., Pablo, G., Cueva, R. & Larriba, G. Screening for new yeast mutants affected in
912 mannosylphosphorylation of cell wall mannoproteins. *Yeast* **20**, 1189–1211 (2003).

913 38. Friis, J. & Ottolenghi, P. The genetically determined binding of alcian blue by a minor fraction
914 of yeast cell walls. *C R Trav Lab Carlsberg* **37**, 327–341 (1970).

915

916 39. Casini, A., Storch, M., Baldwin, G. S. & Ellis, T. Bricks and blueprints: methods and standards
917 for DNA assembly. *Nat Rev Mol Cell Biol* **16**, 568–576 (2015).

918 40. Moore, S. J. *et al.* EcoFlex: A Multifunctional MoClo Kit for *E. coli* Synthetic Biology. *ACS*
919 *Synth. Biol.* **5**, 1059–1069 (2016).

920 41. Lee, M. E., DeLoache, W. C., Cervantes, B. & Dueber, J. E. A Highly Characterized Yeast
921 Toolkit for Modular, Multipart Assembly. *ACS Synth. Biol.* **4**, 975–986 (2015).

922 42. van Dolleweerd, C. J. *et al.* MIDAS: A Modular DNA Assembly System for Synthetic Biology.
923 *ACS Synth. Biol.* **7**, 1018–1029 (2018).

924 43. Hernanz-Koers, M. *et al.* FungalBraid: A GoldenBraid-based modular cloning platform for the
925 assembly and exchange of DNA elements tailored to fungal synthetic biology. *Fungal*
926 *Genetics and Biology* **116**, 51–61 (2018).

927 44. Sarrion-Perdigones, A. *et al.* GoldenBraid: An Iterative Cloning System for Standardized
928 Assembly of Reusable Genetic Modules. *PLoS ONE* **6**, e21622 (2011).

929 45. Obst, U., Lu, T. K. & Sieber, V. A Modular Toolkit for Generating *Pichia pastoris* Secretion
930 Libraries. *ACS Synth. Biol.* **6**, 1016–1025 (2017).

931 46. Andreou, A. I. & Nakayama, N. Mobius Assembly: A versatile Golden-Gate framework
932 towards universal DNA assembly. *PLoS ONE* **13**, e0189892 (2018).

933 47. Engler, C. *et al.* A Golden Gate Modular Cloning Toolbox for Plants. *ACS Synth. Biol.* **3**, 839–
934 843 (2014).

935 48. Weber, E., Engler, C., Gruetzner, R., Werner, S. & Marillonnet, S. A Modular Cloning System
936 for Standardized Assembly of Multigene Constructs. *PLoS ONE* **6**, e16765 (2011).

937 49. Potapov, V. *et al.* Comprehensive Profiling of Four Base Overhang Ligation Fidelity by T4
938 DNA Ligase and Application to DNA Assembly. *ACS Synth Biol* **7**, 2665–2674 (2018).

939 50. OPENPichia plasmid set | BCCM Belgian Coordinated Collections of Microorganisms.
940 <https://bccm.belspo.be/catalogues/plasmid-sets/openpichia>.

941 51. Jungmann, J., Rayner, J. C. & Munro, S. The *Saccharomyces cerevisiae* protein
942 Mnn10p/Bed1p is a subunit of a Golgi mannosyltransferase complex. *J Biol Chem* **274**, 6579–
943 6585 (1999).

944 52. HOC1 Interactions | SGD. <https://www.yeastgenome.org/locus/S000003836/interaction>.

945 53. Wu, L. *et al.* Global catalogue of microorganisms (gcm): a comprehensive database and
946 information retrieval, analysis, and visualization system for microbial resources. *BMC*
947 *Genomics* **14**, 933 (2013).

948 54. Lin, Y.-C. *et al.* Genome dynamics of the human embryonic kidney 293 lineage in response
949 to cell biology manipulations. *Nat Commun* **5**, 4767 (2014).

950 55. Andrews, S. *FastQC: A Quality Control Tool for High Throughput Sequence Data. Available*
951 *online at: http://www.bioinformatics.babraham.ac.uk/projects/fastqc/*. (2010).

952 56. Bolger, A. M., Lohse, M. & Usadel, B. Trimmomatic: a flexible trimmer for Illumina sequence
953 data. *Bioinformatics* **30**, 2114–2120 (2014).

954 57. Kumar, S., Stecher, G., Li, M., Knyaz, C. & Tamura, K. MEGA X: Molecular Evolutionary
955 Genetics Analysis across Computing Platforms. *Molecular Biology and Evolution* **35**, 1547–
956 1549 (2018).

957 58. Heiss, S., Maurer, M., Hahn, R., Mattanovich, D. & Gasser, B. Identification and deletion of
958 the major secreted protein of *Pichia pastoris*. *Applied microbiology and biotechnology* **97**,
959 1241–1249 (2013).

960 59. Näätasaari, L. *et al.* Deletion of the *Pichia pastoris* KU70 Homologue Facilitates Platform Strain
961 Generation for Gene Expression and Synthetic Biology. *PLoS ONE* **7**, e39720 (2012).

962 60. Weninger, A., Hatzl, A.-M., Schmid, C., Vogl, T. & Glieder, A. Combinatorial optimization of
963 CRISPR/Cas9 expression enables precision genome engineering in the methylotrophic yeast
964 *Pichia pastoris*. *Journal of Biotechnology* **235**, 139–149 (2016).

965 61. Wu, S. & Letchworth, G. J. High efficiency transformation by electroporation of *Pichia pastoris*
966 pretreated with lithium acetate and dithiothreitol. *BioTechniques* **36**, 152–154 (2004).

967 62. Livak, K. J. & Schmittgen, T. D. Analysis of relative gene expression data using real-time
968 quantitative PCR and the 2(-Delta Delta C(T)) Method. *Methods* **25**, 402–408 (2001).

969 63. R: The R Project for Statistical Computing. <https://www.r-project.org/>.

970 64. Lüdecke, D. ggeffects: Tidy Data Frames of Marginal Effects from Regression Models. *The*
971 *Journal of Open Source Software* **3**, (2018).

972 65. Zeileis, A., Köll, S. & Graham, N. Various Versatile Variances: An Object-Oriented
973 Implementation of Clustered Covariances in R. *Journal of Statistical Software* **95**, 1–36
974 (2020).

975 66. Hothorn, T., Bretz, F. & Westfall, P. Simultaneous inference in general parametric models.
976 *Biom J* **50**, 346–363 (2008).

977 67. Ram, A. F. J. & Klis, F. M. Identification of fungal cell wall mutants using susceptibility assays
978 based on Calcofluor white and Congo red. *Nat Protoc* **1**, 2253–2256 (2006).

979 68. Arendt, P. *et al.* An endoplasmic reticulum-engineered yeast platform for overproduction of
980 triterpenoids. *Metab Eng* **40**, 165–175 (2017).

981 69. McDonald, K. L. & Webb, R. I. Freeze substitution in 3 hours or less. *J Microsc* **243**, 227–233
982 (2011).

983 70. Walter, M. R. *et al.* Three-dimensional structure of recombinant human granulocyte-
984 macrophage colony-stimulating factor. *Journal of Molecular Biology* **224**, 1075–1085 (1992).

985 71. Wrapp, D. *et al.* Structural Basis for Potent Neutralization of Betacoronaviruses by Single-
986 Domain Camelid Antibodies. *Cell* **181**, 1004–1015.e15 (2020).

987 72. Yang, Z. *et al.* A Novel Multivalent, Single-Domain Antibody Targeting TcdA and TcdB
988 Prevents Fulminant Clostridium difficile Infection in Mice. *The Journal of Infectious Diseases*
989 **210**, 964–972 (2014).

990 73. McPherson, M. J. *et al.* Galactose oxidase of *Dactylium dendroides*. Gene cloning and
991 sequence analysis. *Journal of Biological Chemistry* **267**, 8146–8152 (1992).

992 74. Kubala, M. H., Kovtun, O., Alexandrov, K. & Collins, B. M. Structural and thermodynamic
993 analysis of the GFP:GFP-nanobody complex. *Protein Science* **19**, 2389–2401 (2010).

994

995 **Tables**

996

997 **Table 1. Strains used in this publication.** * Type strain; Abbreviations: UCD: University of California, Davis, USA;
998 CBS: Centraalbureau voor Schimmelcultuuren, currently known as Westerdijk Fungal Biodiversity Institute, The
999 Netherlands; NCYC: National Collection of Yeast Cultures, UK; NRRL: Northern Regional Research Laboratory,
1000 currently known as Agricultural Research Service (ARS), USA; NTG: nitrosoguanidine.

Strain ID	Origin of strain isolate	Source	Original depositor
CBS 2612 *	<i>Quercus kelloggii</i> (California, USA)	CBS culture collection	HJ Phaff, UCD
NCYC 2543 *	<i>Quercus kelloggii</i> (California, USA)	NCYC culture collection	CBS
NRRL YB-4290 *	<i>Quercus kelloggii</i> (California, USA)	NRRL culture collection	HJ Phaff, UCD
NRRL Y-7556 *	<i>Quercus kelloggii</i> (California, USA)	NRRL culture collection	D. Yarrow, CBS
UCD FST K-239 *	<i>Quercus kelloggii</i> (California, USA)	UCD culture collection	HJ Phaff, UCD
NRRL Y-11430	Most likely a subclone of the type strain	NRRL culture collection	Patent deposit Phillips Petroleum Company (USA)
GS115	NTG-mutagenized derivative of NRRL Y-11430	Internal VIB culture collection	
NCYC 2543 <i>his4</i>	Mutagenesis	This publication	
NCYC 2543 <i>hoc1^{tr}-1</i>	Mutagenesis	This publication	
NCYC 2543 <i>hoc1^{tr}-2</i>	Mutagenesis	This publication	

1001

1002 **Table 2. Overview of the functional mutations of the analysed *K. phaffii* strains compared to the CBS 7435**
1003 **(eq. strain deposit of NRRL- Y-11430) reference genome, non-functional SNPs and indels are between brackets.**
1004 **Functional mutations are those resulting in a SNP or indel in a gene.**

Strain Designation	SNP	Indel	Total	Mutations/Mbp	Killer plasmids copy number (KP1/KP2)
NRRL Y-11430	0 (2)	2 (18)	2 (20)	2.3	21/15
NRRL YB-4290	2 (2)	3 (20)	5 (22)	2.9	140/82
NCYC 2543	3 (5)	3 (18)	6 (23)	3.1	none detected
CBS 2612	3 (4)	3 (19)	6 (23)	3.1	none detected
NRRL Y-7556	3 (3)	3 (21)	6 (24)	3.2	138/86

1005

1006
1007
1008
1009
1010
1011
1012
1013

Table 3. Summary of the coding mutations in the Philips Petroleum strain and the type strains, compared to the CBS 7435 reference genome. The exact mutations are mentioned in the second column, with the CBS 7435 amino acid as reference amino acid; although the original genetic makeup is as present in the type strains, and it is the CBS 7435/NRRL Y-11430 that mutated. The mutations indicated with an asterisk were also reported by Brady et. al.²⁴. All mutations found in these strains are concentrated in eight locations. The mutations in *SEF1*, *ROP100/RSF2*, and *HOC1* are shared by all type strains. Two mutations in a gene encoding for a hypothetical protein were found in all sequenced genomes. The other mutations (in *SRB7*, *RAD18* and *PRP46*) are present in one of the type strains, NCYC 2543, CBS 2612 and NRRL Y-7556, respectively.

Gene	Mutation	NRRL Y-11430	NRRL YB-4290	NCYC 2543	CBS 2612	NRRL Y-7556	Gene function
<i>SEF1</i>	SNP: C315S		x	x	x	x	Putative transcription factor
<i>ROP100/RSF2</i>	SNP: *748W		x*	x	x	x*	Methanol- and biotin-starvation-inducible zinc finger protein
<i>HOC1</i>	Indel: (T) ₅₋₆ Premature *		x	x	x	x	Alpha1,6mannosyltransferase
Hypothetical	Indel 1: +G Indel 2: +GT GNYD821GFPND	x	x	x	x	x	Papain-like cysteine protease
<i>SRB7</i>	SNP: E131Q			x			RNA polymerase II mediator complex subunit
<i>RAD18</i>	SNP: K210N				x		E3 ubiquitin ligase
<i>PRP46</i>	SNP: Q320L					x	NineTeen Complex (NTC) component
Total mutations in protein-coding sequences		2	5	6	6	6	

1014

1015

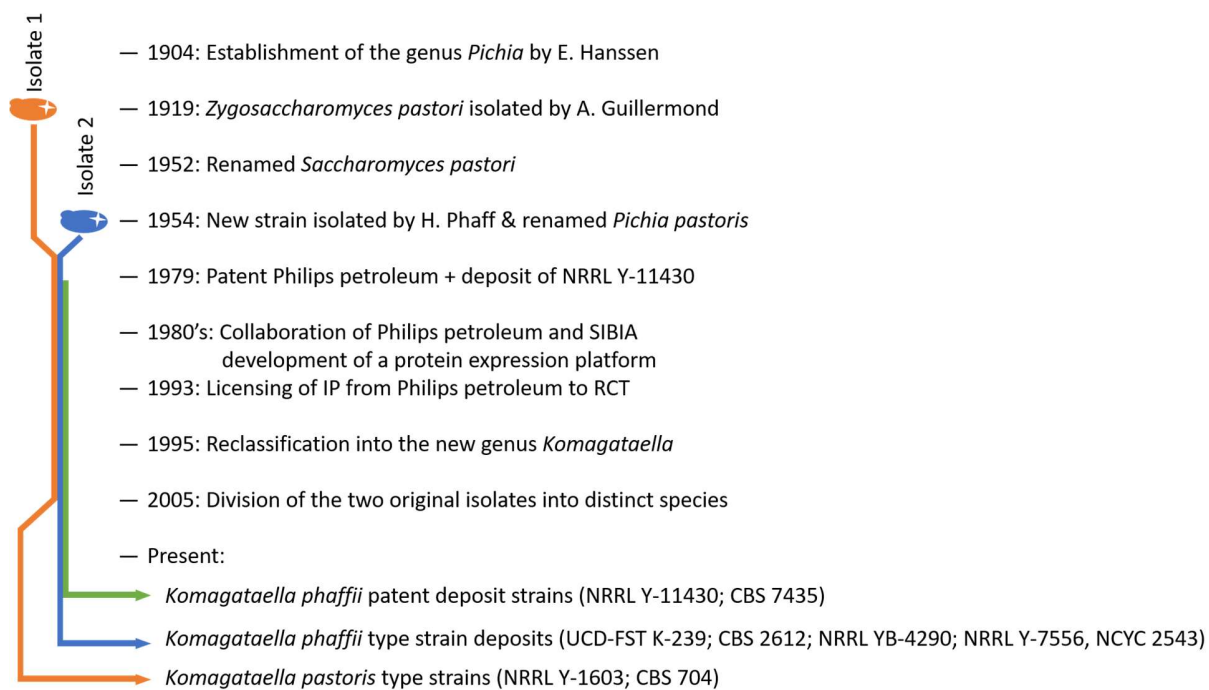
Table 4. Details of the selected proteins used for the protein expression comparisons.

Abbreviation	Name	Type	Molecular mass (kDa)	Secretion leader	Ref.
GM-CSF	Granulocyte-macrophage colony-stimulating factor	Cytokine	15.7	αMF	70
GaOx	Galactose oxidase from <i>Fusarium graminearum</i>	Enzyme	69.9	αMF	73
Cdiff-VHH-IgA	Anti- <i>C. difficile</i> toxin VHH IgA fusion protein	VHH-IgA	41.2	Ost1	72
CovidVHH-IgG	SARS-CoV-2 neutralizing VHH hIgG1 fusion protein	VHH-IgG	40.6	Ost1	71
GBP	<i>GFP-binding protein</i>	VHH	14.1	MF	74

1016

1017 **Figures**

1018

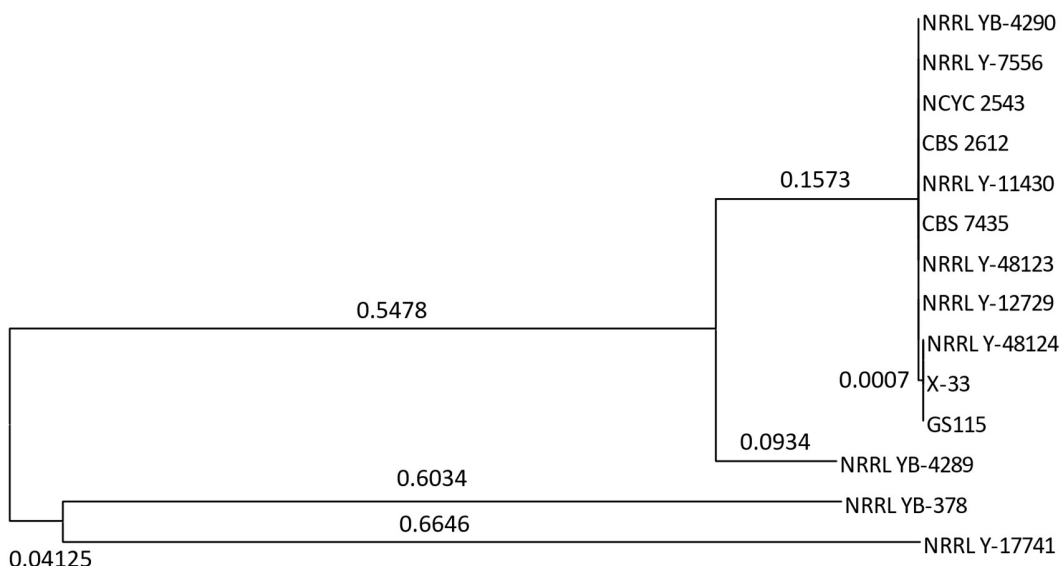


1019

1020 **Figure 1. Schematic timeline of the history of the *Komagataella* species and the available type strain deposits**

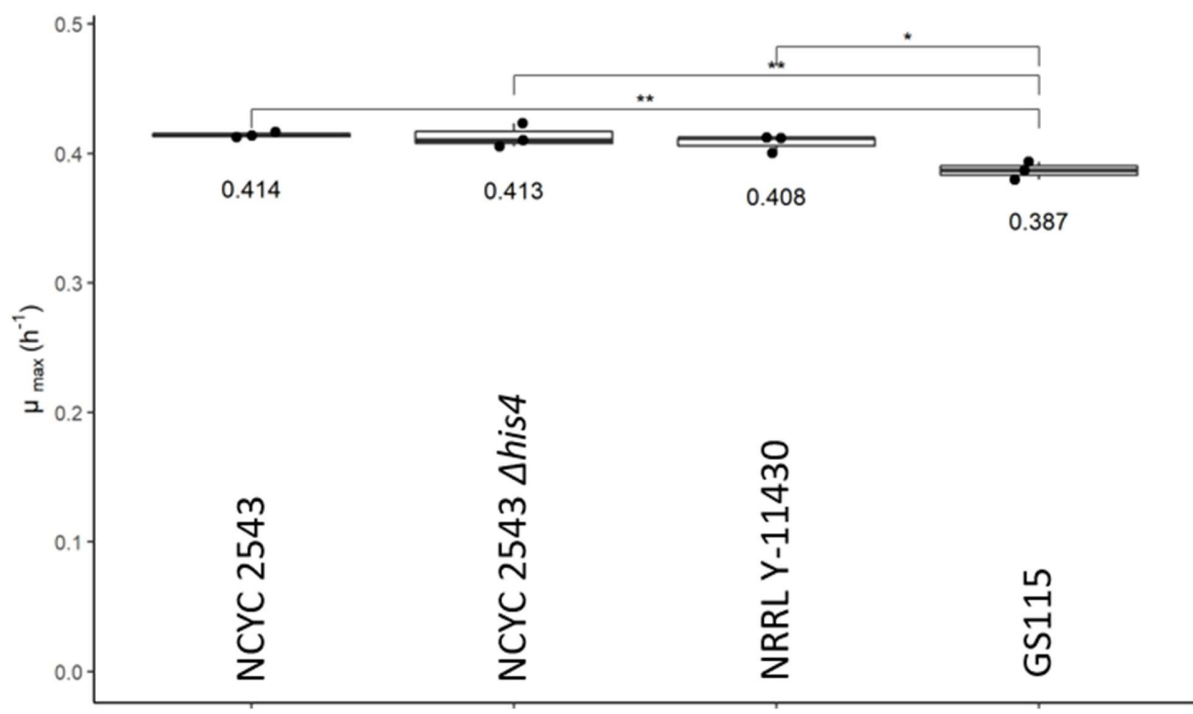
1021 **and patent strain deposits.**

1022



1023
1024 **Figure 1: Phylogenetic tree of the *K. phaffii* strains with node lengths.** The tree was constructed using a Maximum

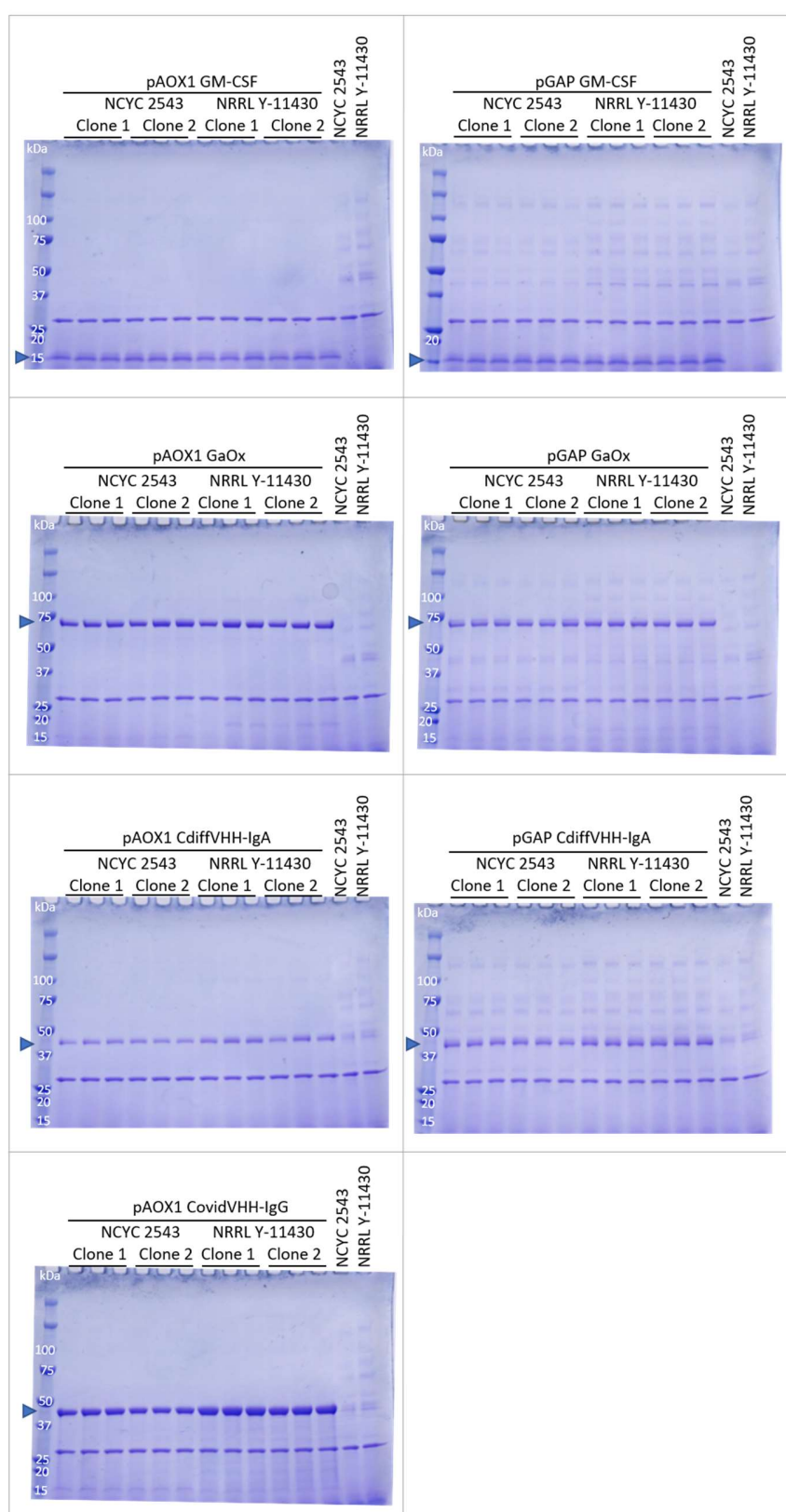
1025 Likelihood method and Hasegawa-Kishino-Yano model. Node lengths of less than 0.0001 were neglected.



1026

1027
1028
1029
1030

Figure 3. Maximum growth rate of the different *Pichia* strains, plotted individually as dots, as well as a boxplot with median value. A one-way ANOVA test showed significant influence of the strain on the growth rate ($p = 0.0034$). A post-hoc Tukey test shows that GS115 grows significantly slower than the other strains. The asterisks indicate the p-value of the Tukey test: **, $0.01 > p > 0.001$; *, $0.05 > p > 0.01$.



1031
1032
1033
1034
1035

Figure 4. Expression comparison between NCYC 2543 and NRRL Y-11430. The proteins were expressed using the GAP or AOX1 promoter. As controls, both wild type strains were grown and analysed as well. Supernatant samples were treated with EndoH to remove N-glycans and samples were analysed on SDS-PAGE. EndoH is also visible on the gels at around 30 kDa.

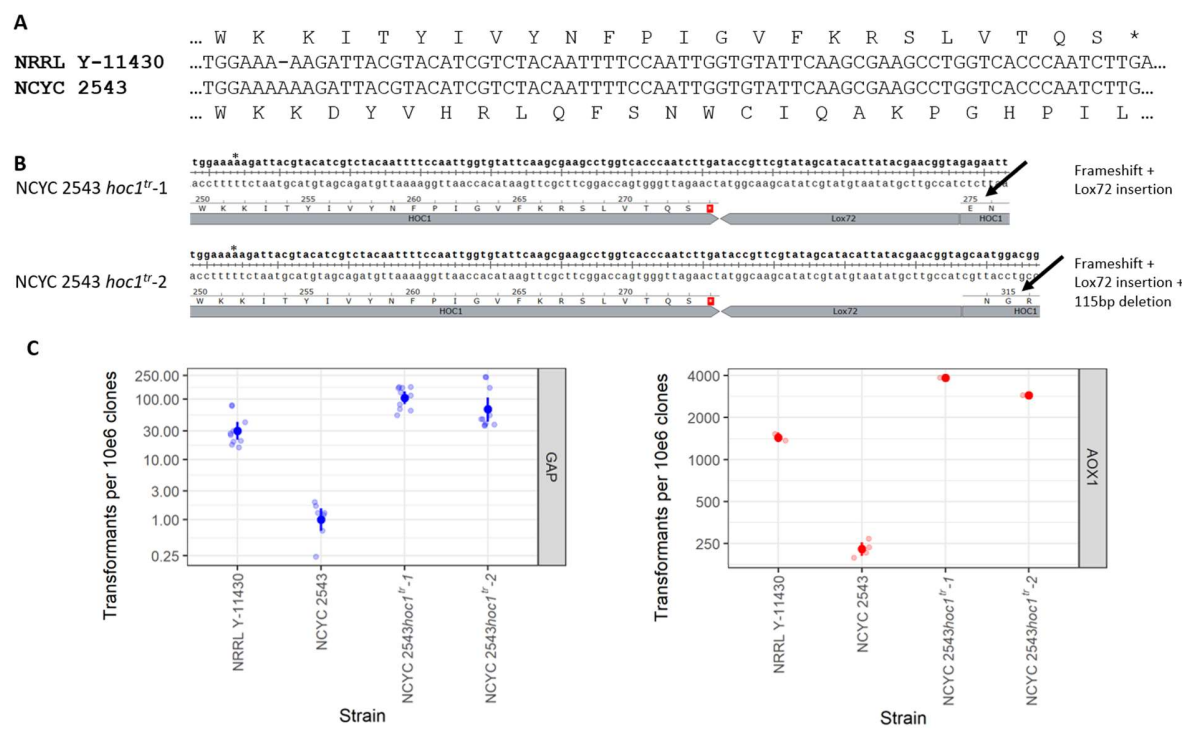
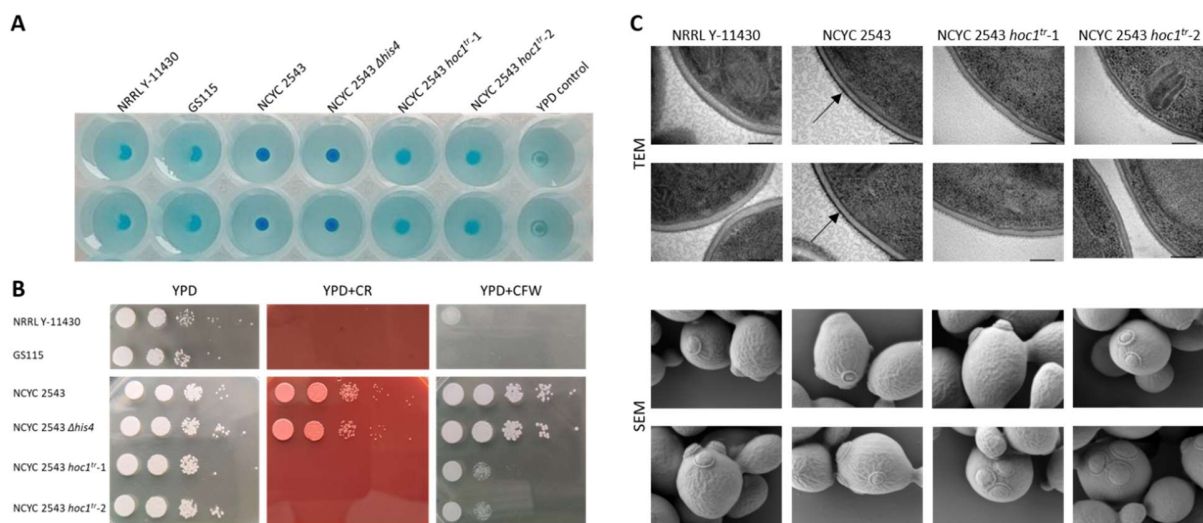
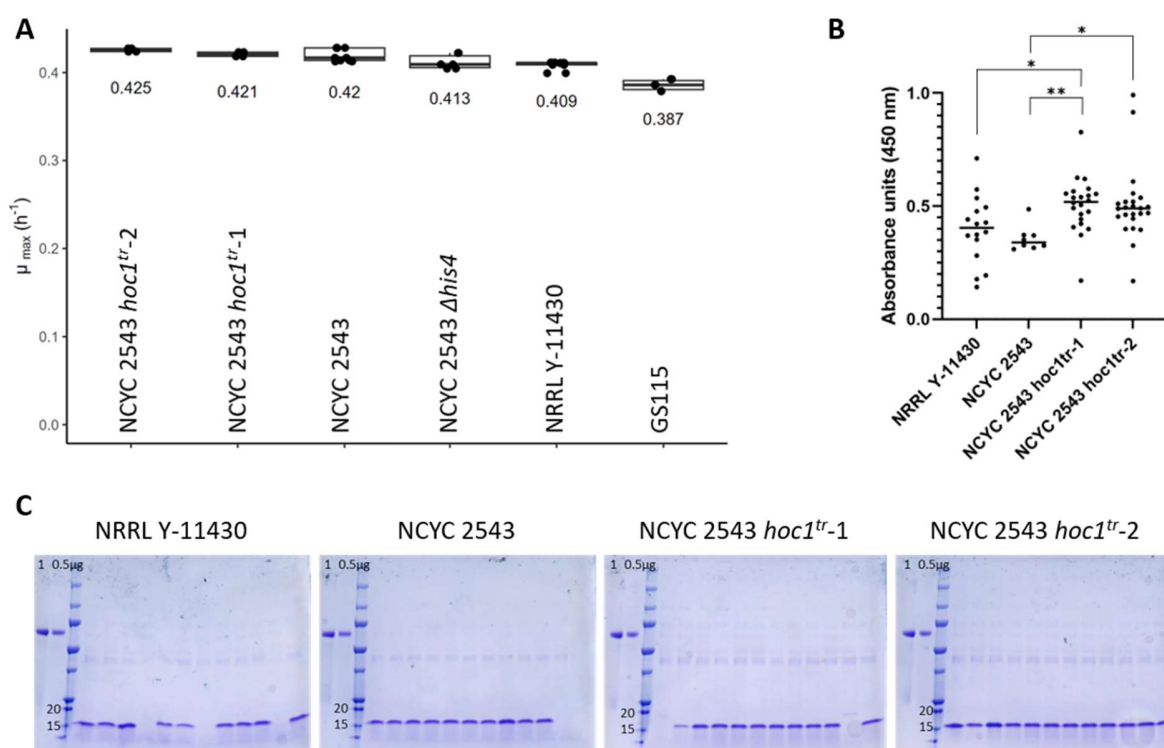


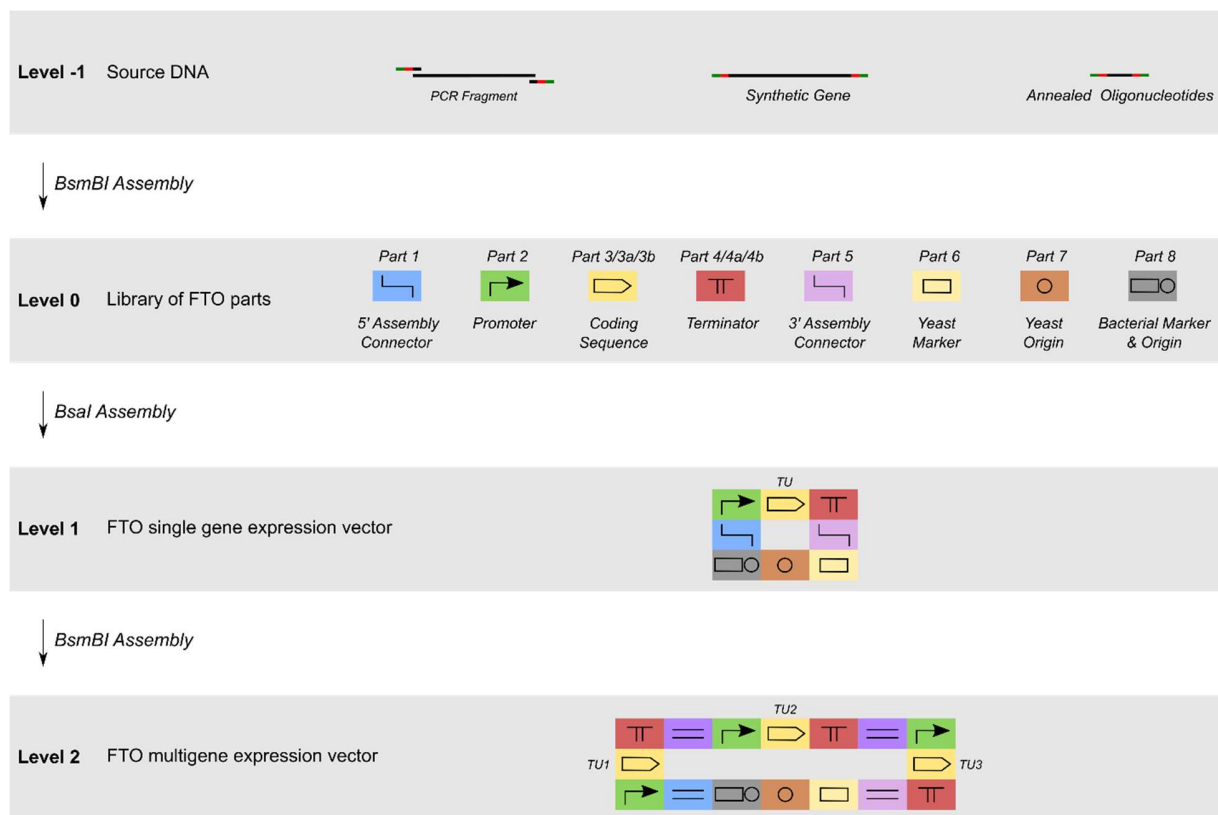
Figure 5. Overview of the HOC1 genome engineering strategy and the effect on transformation efficiency of the resulting strains. A. Alignment of a part of the HOC1 gene as present in NRRL Y-11430 vs. NCYC 2543, showing the frameshift resulting in a premature stop codon in the NRRL Y-11430. B. Resulting genomic HOC1 sequence upon split-marker-based gene editing. Two strategies were followed, where either the single base pair deletion (indicated with *) resulting in the *Hoc1p* truncation and a Lox72 scar is introduced downstream of the stop codon; or where an additional 115 bp deletion downstream of the resulting stop codon and Lox72 scar is introduced. C. Transformation efficiency in the two wild type strains and two HOC1-engineered strains, either using a pGAP-based plasmid (left) or a pAOX1-based plasmid (right). The analysis was performed as described in the Materials & Methods section.



1046 **Figure 6. Characterization of the cell walls of NRRL Y-11430, NCYC 2543 and the two NCYC 2543 *hoc1^{tr}* mutants.**
1047 A. Alcian blue staining of the strains to determine the density of negative charges at the yeast cell wall. Alcian blue is
1048 a cationic dye that binds negative charges at the cell wall. The more intense the blue staining of the cells, the more
1049 negative charge, i.e., mannosylphosphate moieties, are present on the glycan trees of the cell wall mannoproteins.
1050 Duplicate wells are shown per strain (vertical). B. Sensitivity of the strains towards Congo red and Calcofluor white,
1051 compared to growth on YPD agar, as an indicator for cell wall integrity. The plates were incubated for 3 days at 30 °C.
1052 C. Transmission electron microscopy (TEM) and scanning electron microscopy (SEM) images of the four strains. The
1053 increased electron density of the outermost layer, i.e., the cell wall is indicated with an arrow in the TEM images of the
1054 NCYC 2543 strain. Only two individual images per strain are shown.



1055
1056 **Figure 7. Overview of the strain performance of NRRL Y-11430, NCYC 2543 and the two NCYC 2543/OPENPichia**
1057 ***hoc1^{tr}* mutants.** A. Comparison of the maximal growth rate of the four main strains, accompanied by GS115 and the
1058 NCYC 2543/OPENPichia *his4*. B. ELISA results of 24 clones of pGAP-based GBP expression in the different strains
1059 (no selection for single copies was done, wells were excluded when no expression was observed on SDS-PAGE,
1060 assuming these clones contain no expression cassette, or due to a technical issue during the ELISA procedure).
1061 Absorbance units were background corrected. All strains were compared in a Kruskal-Wallis omnibus test, followed by
1062 pairwise comparison corrected with Dunn's multiple comparison procedure. Significance scores are annotated as
1063 follows, *: 0.002 < p < 0.03; **: 0.001 < p < 0.002; non-significant differences are not shown. C. SDS-PAGE analysis of the
1064 first 12 clones per transformation. Equal volumes of supernatant were loaded.



1065

1066 **Figure 8. The modular cloning or MoClo principle.** In a first phase, source DNA, such as PCR fragments, synthetic
 1067 genes or annealed oligonucleotides are flanked with the proper Type IIS restriction sites and 4 nt overhangs, which are
 1068 then accommodated in a Level 0 entry vector through *BsmBI* digest and T4 DNA ligation. Then, selected Level 0 vectors
 1069 are assembled into a Level 1 expression vector by means of a *BsaI* digest and T4 DNA ligation. Finally, the system
 1070 allows the assembly of multiple transcription units (promoter, CDS, terminator) from the individual Level 1 vectors, into
 1071 a higher order Level 2 vector, in case the assembly connector sequences were properly selected during the assembly
 1072 of the Level 1 vectors. Assembled assembly connectors are depicted with two horizontal lines and different shades of
 1073 blue and purple. Note that the Part 3 Coding Sequence can be split up in a Part 3a and Part 3b Coding Sequence, to
 1074 allow additional modularity. Likewise, the Part 4 Terminator can be split up in a Part 4a Coding Sequence and a Part
 1075 4b Terminator. Figure adapted from Lee et al⁴¹.